OPTIMAL LOCATION OF PV POWERED SMART CHARGING FACILITIES WITH ENERGY STORAGE FOR ELECTRIC VEHICLES

A Thesis

Presented to

the Faculty of the Department of Electrical and Computer Engineering

University of Houston

In Partial Fulfillment

of the Requirements for the Degree

Master of Science

in Electrical Engineering

by

Michael Umeano

August 2016

OPTIMAL LOCATION OF PV POWERED SMART CHARGING FACILITIES WITH ENERGY STORAGE FOR ELECTRIC VEHICLES

Michael Umeano

Approved:

Chair of the Committee
Dr. Wajiha Shireen, Professor,
Electrical and Computer Engineering,
Engineering Technology

Committee Members:

Dr. Zhu Han, Professor,
Electrical and Computer Engineering

Dr. Miao Pan, Assistant Professor,
Electrical and Computer Engineering,

Dr. Masoud Barati, Instructional
Professor, Electrical and Computer
Engineering,

Dr. Jung UK Lim, Instructional
Professor, Electrical and Computer
Engineering

Dr. Suresh K. Khator, Associate Dean,
Cullen College of Engineering

Dr. Badri Roysam, Professor and Chair,
Electrical and Computer Engineering

Acknowledgements

I wish to thank the following people: Dr Wajiha Shireen, for the support, patience and encouragement towards my work; Dr.Preetham Goli, for the immense help with bringing me up to speed in a field I was unfamiliar with; My good parents and siblings for giving me this priceless opportunity to study further and the encouraging words during difficult times; I thank Dr. Jung UK Lim, Dr. Aaron Becker, and Dr. Masoud Barati, for all the meetings we held to improve my research skills and contributions to my thesis technical content; Thanks to Abraham Oladejo, Nicholas Hernandez, Olumide Esho and Rikesh Shah for all the fun we had in the lab brainstorming together.

There are a lot more people I would thank, but space and their modesty compel me to stop here.

OPTIMAL LOCATION OF PV POWERED SMART CHARGING FACILITIES WITH ENERGY STORAGE FOR ELECTRIC VEHICLES

An Abstract

of a

Thesis

Presented to

the Faculty of the Department of Electrical and Computer Engineering

University of Houston

In Partial Fulfillment

of the Requirements for the Degree

Master of Science

in Electrical Engineering

by

Michael Umeano

August 2016

Abstract

Increasing charging facilities to service electric vehicles (EVs) and Plug-in Hybrid Electric Vehicles (PHEVs) leads to increased stress on the existing electric grid. PV integrated charging stations (PVCS) supplemented with energy storage have provided promising results in reducing dependency on the electric grid for charging PHEVs. Despite advances in power electronics used to interface PVCS with the grid, random charging patterns, structural contingencies and intermittency of solar energy creates the inevitable issue of random power penetration and adoption to/from the grid. To maximize the benefits of PVCS they should be integrated into the distribution network at optimum locations. A well planned and operated PVCS would provide several benefits to the distribution network such as reduction in power losses, voltage regulation and reactive power support. This paper proposes a new method for optimally siting PV powered PHEV charging facilities with energy storage in a distribution network under stress due to heavy penetration of PHEVs. The performance of the proposed heuristic method is demonstrated through a case study using an IEEE 30-bus system.

Table of Contents

List of Figures

List of Tables

Chapter 1 Introduction

1.1 Introduction

Global awareness for a pollution free environment has driven the utilities towards sustainable solutions for electricity generation. This has in turn led to the rapid deployment of alternative energy resources such as photovoltaics (PV) into the distribution network. Simultaneously the transportation sector has witnessed a steady rise in electrified vehicles with major automotive manufacturers introducing electric vehicles (EVs) and plug-in hybrid electric vehicles (PHEVs) into the market. The proliferation of PHEVs requires charging stations to fulfill their battery requirements. Though PHEVs are being marketed with the goal of minimizing the pollution from automobiles, the energy requirements for charging the batteries is still met by power generated from fossil fuel sources. Public charging of PHEVs, in particular DC fast charging, will lead to excessive loading of power delivery equipment and fluctuations in feeder/bus voltages, stressing the distribution network. Smart charging stations integrated with PV generators and energy storage are proposed as viable solutions to mitigate the above issues.

Large-scale penetration of PHEVs have the propensity to cause detrimental and destabilizing effects on the electric power grid [1]. With variations in load demands, power production tends to vary significantly. Since the initial deployment of PHEVs is assumed to be clustered to a particular neighborhood, research has been focused on the impact felt on the distribution network during PHEV charging [2]. Depending on the time of charge, charging location, charging methods and charging power levels there could be several ramifications on the distribution network. The likelihood of observing local distribution infrastructure inadequacies significantly increases as higher voltages are used to reduce charging duration. Figure 1.1 illustrates the impact that one, two, or three PHEVs will have on a single distribution transformer rated at 50 kVA during peak summer loading period.

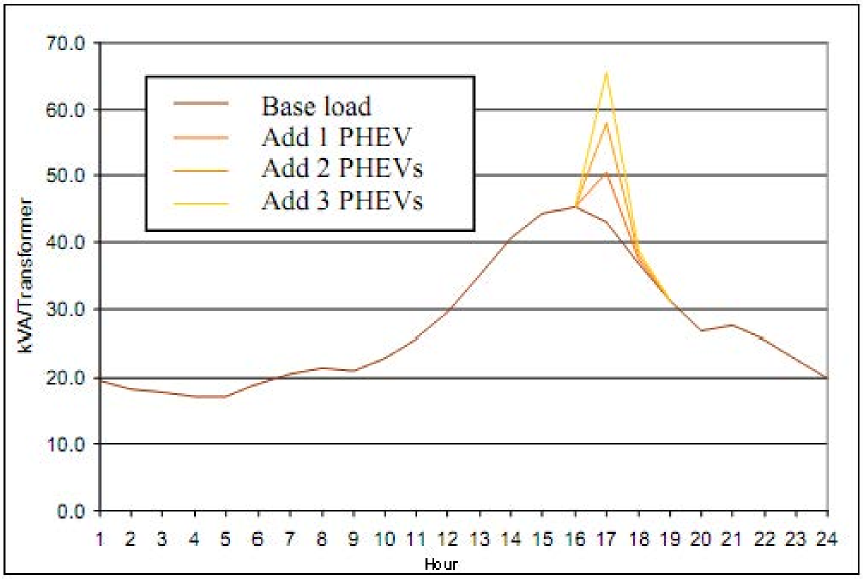

Figure 1.1: Impact of Aggressive PHEV Penetration on Peak Summer Transformer Loads

To facilitate the high penetration levels of PHEVs without much adverse impact on the distribution equipment current research recommends the installation of PV integrated charging facilities (PVCFs) [3,4]. However, during the periods of high PV generation and low PHEV load conditions an anti-islanded PV charging facility may cause adverse situations on the grid such as voltage rise, sags, flicker, power flow inversion and voltage frequency fluctuations. Figure 1.2 shows an example of reverse power flow condition with the proliferation of PV-DG. Penetration levels over a 24 h period follow power delivery trends similar to power delivered from solar insolation on a typical day. In addition to this, coordination of distribution system components such as voltage regulators and protection systems introduce additional challenges. Since the distribution equipment are at an increasing risk of maloperation, these issues require close attention with the increasing penetration of PVCFs.

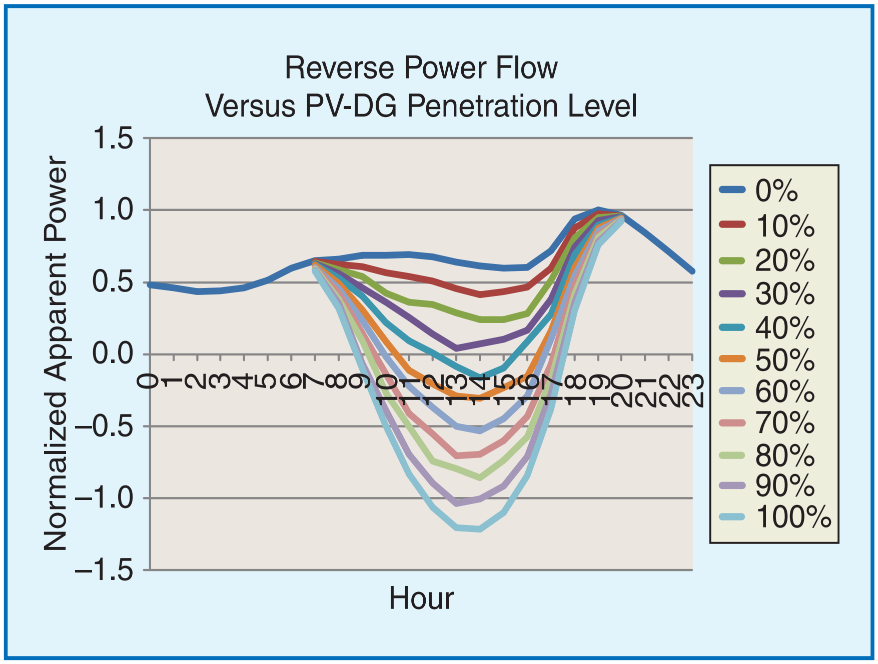

Figure 1.2: Reverse power flow for various penetration levels of PV-DG

1.2 Research Motivation and Objectives

Literature has shown that without additional electric source from DG's or energy storage in a microgrid, the current electrical infrastructure will impede the installation of EV charging stations and EV charging. Although the cost of energy from conventional sources is generally lower than that of renewable energy sources, an optimal combination of electric power from renewable energies and fossil fuels can reduce the overall cost of charging PHEVs. However, the installation of PVCFs at inappropriate locations could lead to negative effects on the distribution systems concerned, such as relay system configurations, voltage profiles, and network losses. Due to the stochastic nature of the solar energy resource and PHEV loads it becomes imperative to have an energy storage unit (ESU) for managing power flow in a PVCF [5].

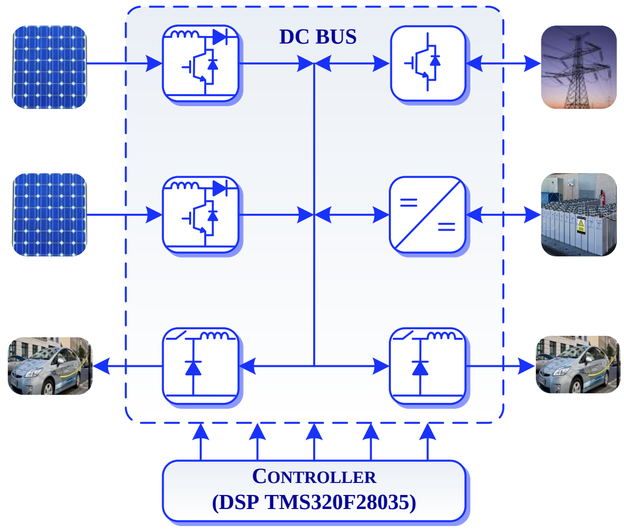

Figure 1.3: Architecture of the PV integrated charging facility

PHEVs in the charging station can be coordinated with the ESU and PV to provide voltage support for the distribution feeders. To maximize the benefits of PVCFs they should be integrated into the distribution network at optimum locations [6,7]. A well planned and operated PVCF could provide several benefits to the distribution network such as reduction of power losses, voltage regulation and reactive power support. In view of this, this thesis proposes an algorithm dedicated to the optimal placement of PVCFs in a given distribution system with random PHEV charging patterns. Based on the existing data for PV irradiation and PHEV charging load, PVCF with energy storage is modeled in Matlab/Simulink. The architecture considered for modeling the PVCF is showing in Figure 1.3. Data collected from the model is employed to develop a multi-objective optimization problem that determines an optimal location for installing the PVCF. The optimization problem focuses on reducing power losses, improving voltage stability of the system and indirectly reducing the charging costs of EVs. The performance of the proposed method is demonstrated through a case study using an IEEE 30-

bus microgrid.

The contributions of this thesis can be summarized as follows :

1. Increasing the penetration of PVCF while mitigating adverse impacts on the distribution network.

2. Proposing an algorithm with the goal of preventing high capital cost associated with upgrades to already existing distribution systems equipment in order to accommodate the increase in PVCFs

3. Directly increasing the distance traveled by PHEVs on clean renewable energy, and potentially reducing the size of their battery requirements.

4. Reduction in power losses and voltage drop magnitudes in distribution systems during periods of high PHEV penetration.

1.3 Thesis Organization

The contents of this thesis have been organized in the following manner.

Chapter 1 provides an introduction on the necessity of optimal location for PVCFs in a distribution network. The adverse impacts on the distribution system due to high penetration of PHEVs and PV are highlighted. Problem statement and the proposed solution are briefly described and the motivation and contributions of the thesis are presented.

Chapter 2 covers the detailed literature review on the current knowledge on PV integrated charging facilities. Proposed and existing architectures for PVCFs are reviewed. The impact of high PV penetration on the distribution network is discussed in detail. Finally the need to determine the optimal location of a PVCF with energy storage is discussed.

Chapter 3 describes the detailed model of the PV based charging facility used in this work. The assumptions made, role of the battery controller and the battery control algorithm are shown and justified. The proposed model has been simulated using the simpowersystems toolbox of Matlab/Simulink and the results are presented.

Chapter 4 elaborates on the proposed optimal siting solution. The proposed multi-objective optimization algorithm and the IEEE 30 bus Case on which the developed algorithm would be implemented on are discussed. The feasibility of the proposed method was verified on the IEEE 30 bus Case and the results from Matlab simulations are presented.

Chapter 5 is the concluding chapter which summarizes the contribution of this research and provides some suggestions for future work.

Chapter 2 Literature Review

This chapter presents detailed literature review on PV integrated charging facilities. Proposed and existing architectures for PVCFs are discussed. The impact of high PV penetration on the distribution network also outlined in detail. Finally the need and benefits of placing the PVCF's with energy storage at an optimal node on the grid is presented.

2.1 Introduction

The utilization of energy storage in form of batteries with solar power generation for continous power supply is ubiquitous. They are reliable sources for charging vehicles such as golf carts, scooters and utility vehicles at airports, educational institutions, workplaces etc. [8]. Figure 2.1 shows a picture of such a charging station. The feasibiltiy of a large-scale deployment of photovoltaic chargers in parking lots is analyzed in [9]. A 2.1 kW photovoltaic charging station integrated with the utility at Santa Monica is described in [10]. An experimental control strategy for electric vehicle charging system composed of photovoltaic array, emulated power grid and programmable dc electronic load representing lithium ion battery emulator is presented in [11]. PV parking lot charging and other business models to charge EVs with solar energy are discussed in [12]. Economics of PV powered workplace charging station has been studied in [13] and [14]. The analysis shows the feasibility of a PV based workplace parking garage with benefits to the vehicle owner as compared to home charging, such that the garage owner will get the payback of installations and maintenance cost and profit within the lifetime of the PV panels. According to [14] integrating a solar collector into a parking lot would result in a much more rapid payback-period, encouraging widespread installation of solar capacity. Reference [15] describes how smart control strategies can help PHEVs and PV to integrate with the present electricity system. Co-benefits of large scale deployment of PHEVs and PV systems has been studied in [16]. The study concludes that PVs provides a potential source of midday generation capacity for PHEVs, while PHEVs provide a dispatchable load for low value or otherwise unusable PV generation during periods of low demand (particularly in the spring).

Figure 2.1: PV Based Parking Lot for PHEVs

As per the National household travel survey, vehicles are parked for at least 5 hrs in workplaces [17]. Hence these places are favorable for developing charging station infrastructure but this would lead to serious overloading issues at the distribution level. Since upgrading of transformers is an expensive option for the utilities, this issue needs close attention as the PHEV penetration increases. Several papers have been published to address the overloading of distribution transformers while charging the PHEVs [18–20]. Nevertheless, not much study has been reported to be tightly related to the case of reducing the loading on distribution transformers using a photovoltaic system. Though few papers exist in the literature, they are mostly confined to residential distribution networks [21, 22]. There is plenty of parking area in the U.S - a reasonable fraction of which is suitable for PV installation. Determining the size and type of PV panel is an important criterion for installing a solar carport. Few papers [23], [24] have recommended the use of mono-crystalline silicon as the most cost-effective solar cell type for PV charging facilities. Table 2.1 shows the PV characteristics of various modules, the peak energy produced and the cost of the PV module. The PV panel can be sized by taking the best and worst months into consideration. As described in [25], the initial cost of the PV panel would be $20000 when it is designed based on the worst month of the year and $10000 when it is designed based on the best month of the year. However, for the first case, surplus energy can be injected into the grid, to balance the final cost.

Table 2.1: PV Characteristics

PV Type	**Module Price ($/Wp)**	**Efficiency (%)**	**Peak Energy (Wp)**	**Cost of PV ($)**
Mono-crystalline Silicon	2.14	22	264	565
Polycrystalline Silicon	1.74	15.5	186	324
Thin Film	0.93	12	144	134

Over the years, several configurations for PV based charging facilities have been proposed. The most prominent is the combination of PV and the grid, which is referred as grid-connected PV charging. It uses the PV power whenever possible, but switches to the grid when the PV power is insufficient or unavailable. Another approach is to charge the PHEVs using PV without any support from the grid, which is know as standalone PV charging. There are several variations for this approach, with the inclusion of other power sources such as fuel cell and auxiliary storage. In addition, efforts have also been made to integrate the PV modules/cells on to the body of the PHEV itself.

2.2 Overview of PHEV and PV Technologies

2.2.1 PHEV and Battery

EV (electric vehicle) is widely referred to an electrically powered vehicle which uses one or more motors for its propulsion. The terminology for EV also includes hybrid electric vehicle (HEV) and plug-in hybird electric vehicle (PHEV). In charging context, the main difference between the PHEV/pure EV is that it provides plugs that allow for external charging, while the HEV does not. The HEV charges its battery internally by the kinetics of its combustion engine. The evolution of the EV propulsion battery began with the lead-acid, progressing to nickel and currently to lithium. Modern EVs are no longer using the lead-acid due to its low specific energy, chemical leakage and poor temperature characteristics. They have since been replaced by nickel and now, almost exclusively lithium . Lithium battery is the preferable choice due to its higher energy efficiency, power density, compact and lighter weight. Moreover, it provides fast charging capability, wide operating temperature range, no memory effect, long cycle life and low self-discharge rate. Currently, lithium-based battery includes a wide diversity of chemical substances; for instance, the lithium ferro phosphate ($LiFePO_4$) provides ease in term of handling due to its superior thermal stability in the fully charged condition. In addition it has a low risk of explosion when accidentally over charged or short circuited. Lithium-titanate (LTO) is the latest type, which provides a wider operating temperature range, faster to recharge and accepts higher recharge rate.

2.2.2 PV System

The most widely used PV modules are based on poly or monocrystalline technology. However, recently, thin film is getting popular, especially for large installations. For PHEV charging applications, the modules are arranged in series strings to achieve the required dc bus voltage. To increase the power, several strings are connected in parallel to form an array. The behavior of a PV system under varying irradiance (G) and temperature (T) can be understood by examining its current-voltage (I-V) and power-voltage (P-V) characteristics shown in Figures 2.2 and 2.3. At any time, there exists a unique operating point at which the power is at peak, i.e. the maximum power point (MPP). Naturally, the MPP is not fixed; it fluctuates continuously as G or T varies. Due to these dynamics, the MPP tracker (MPPT) is needed to ensure the maximum power is always extracted from the array.

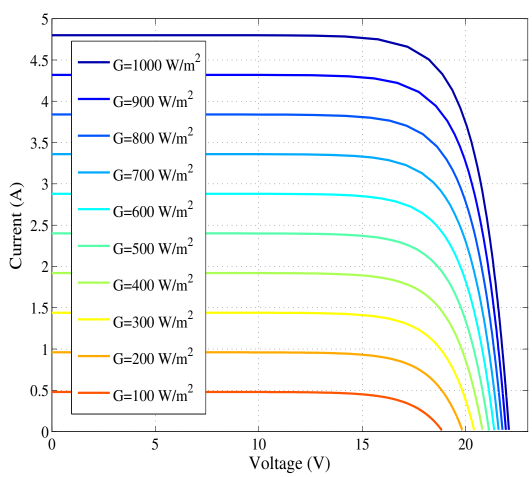

Figure 2.2: I-V Curves at various insolation levels

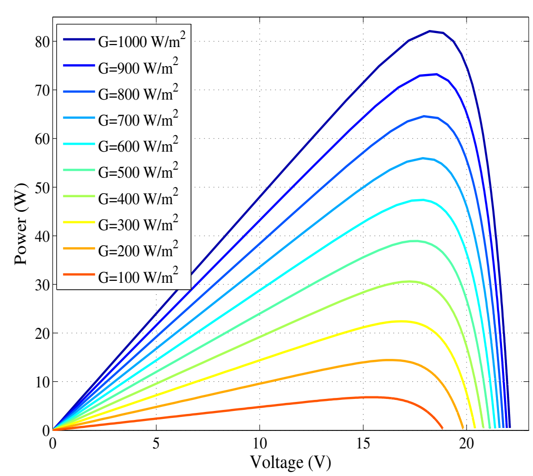

Figure 2.3: P-V Curves at various insolation levels

Invariably, PHEV charging imposes an additional load on the electrical utility system due to the large current it draws from the grid. Furthermore, if the charging takes place during peak hours, the owner may have to pay a high premium for the tariff. To offset this burden, PV charging facilities provide a viable solution to reduce the utility's spinning reserve and improve the grid stability. It is also expected to have a major influence in the smart grid system, which is envisaged to dominate the future power system topology. Currently, two charging approaches using PV, namely the grid-connected PV and standalone PV charging, are known. The PV-grid charging has one major advantage: during insufficient irradiance, the PHEV can be continuously charged by deriving the power from the grid. It is also more flexible because in the absence of PHEV (to be charged) the PV power can be injected to the utility. On the other hand, the PV-standalone is convenient in remote areas where utility supply is not available or too costly. More recently, the hybridization of standalone chargers with secondary power sources such as fuel cell and auxiliary battery are introduced. It must be noted that using PV, the PHEV is charged with dc, which means it needs to bypass Level 1 and Level 2 charging (12 A, 120V and 16 A, 240 V respectively).

2.3 Grid-Connected PV Charging

A typical grid-tied PHEV charging system is shown in Figure 2.4. It has three main components, namely 1) a dc-dc power converter with a built-in MPPT, 2) a bi-directional dc charger and 3) a bi-directional dc-ac inverter. A common dc bus (200-500 Vdc) provides a convenient point for the integration of these components. Crucially, a central controller (microcontroller or C2000 DSP) is required to decide the direction of power flow and switching action of the converters. The operation of the controller is based on intelligent decision making algorithms. It is primarily governed by certain objective functions, for example minimum charging cost, maximum profit etc.

2.3.1 Charging Facility Modes of Operation

When the PHEV is first plugged in, its battery's state of charge (SOC) is normally less than 100%. The central controller commands the charging processes

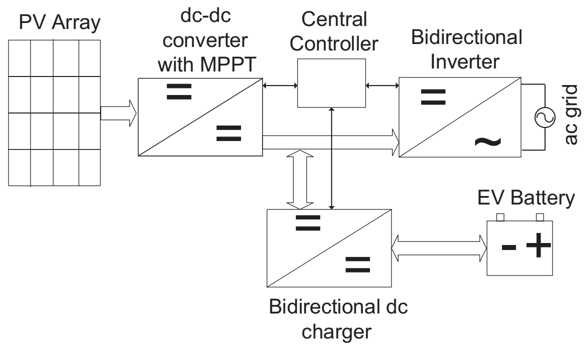

Figure 2.4: Block Diagram of Grid-Connected PV Charging System

based on the condition of the PHEV battery, the availability of PV power and the price of the grid electricity. In general, the PV charging facility (PCF) operates in one of these five modes:

Mode 1 (PV Charging Only)

If the PV energy is sufficient to charge the PHEV, the charging is entirely done by the PV. It is carried out via the dc-dc converter with MPPT and dc charger, as shown in Figure 2.5(a). In this case, the charging system is electrically disconnected from the grid. The dc charger is used to regulate the dc bus voltage to suit the charging profile of a particular PHEV.

Mode 2 (Charging from grid only: Inverter in rectification mode)

On the other extreme, if the PV is totally incapable of supplying any power (in the case of zero or extremely low irradiance), the PHEV will be charged directly from the grid. The ac power is first converted to dc using the bi-directional inverter, operated in the rectification mode. The dc bus voltage is further conditioned by the dc charger to suit the PHEV voltage. This situation is shown in Figure 2.5(b).

Mode 3 (Charging from grid and PV: Inverter in rectification mode)

In cases where the PV is able to deliver certain portion of energy (but not sufficient for full independent charging), then both the PV and grid contribute to the charging, as shown in Figure 2.5(c). Typically, the amount of energy derived from the grid depends on how much energy the PV can deliver. The deficit will be

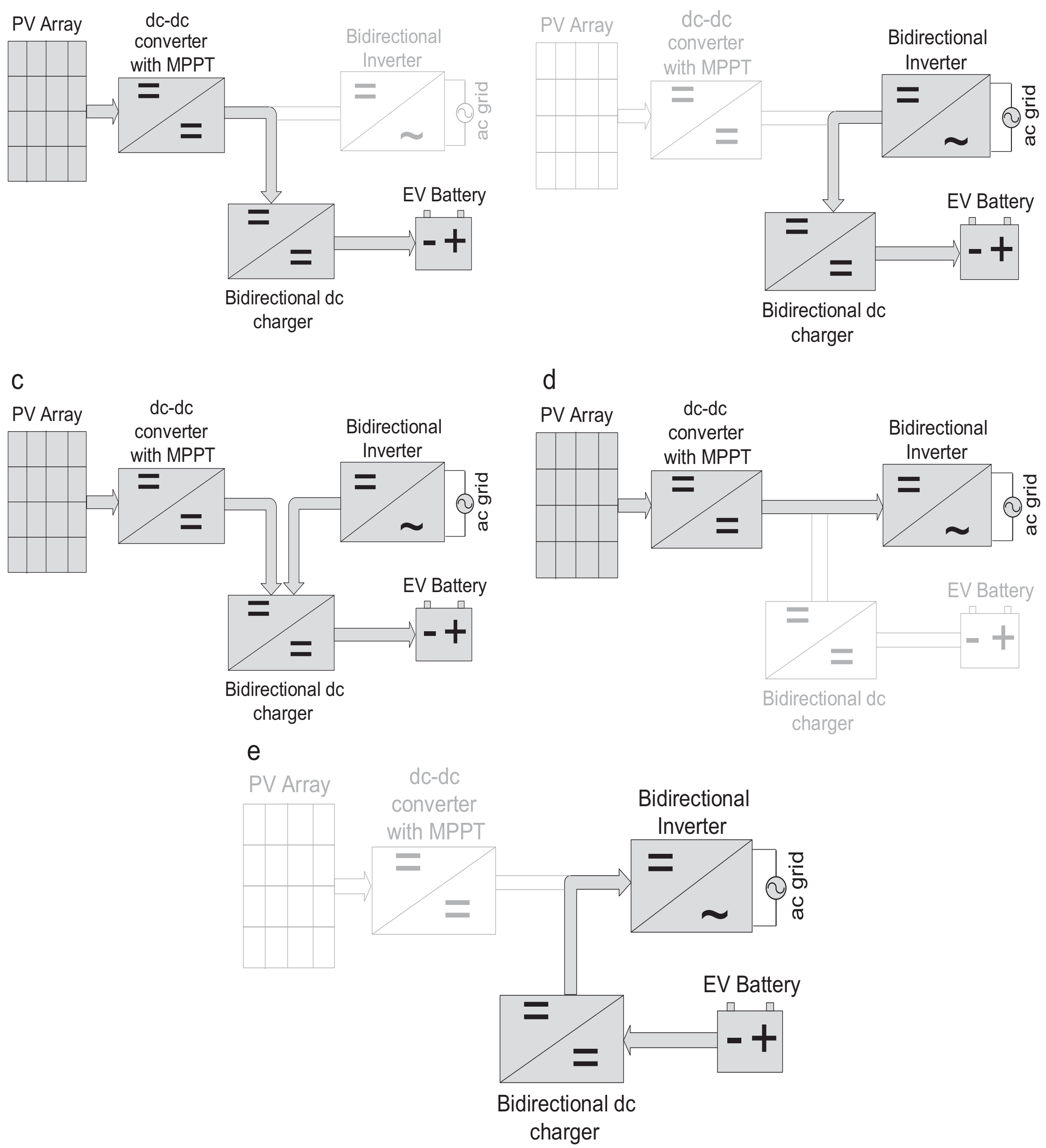

Figure 2.5: PV Charging Facility Modes of Operation

fulfilled by the grid. Obviously, since the irradiance conditions are very dynamic, the controller has to continuously monitor the power delivered by the PV and accordingly adjust the intake from the grid to ensure that the required power to the PHEV is sustained.

Mode 4 (Grid-connected PV: Inverter in inversion mode)

When no PHEV is available for charging and the PV is generating power, all the energy is sold to the grid via two step conversion processes, i.e. by the MPPT dc-dc converter and the bi-directional inverter in inversion mode. This operation is shown in Figure 2.5(d). In certain situations, it may be more economical to operate in this mode, even if the PHEV is available for charging. This is when the feed-in-tariff rate is much higher that makes such proposition viable.

Mode 5 (Vehicle to grid: Inverter in inversion mode)

In this mode, the idea of transferring the power from vehicle to grid (V2G) is introduced. In certain hours of the day, the tariff is very high; thus if there is surplus energy from the PHEV that is standing idly in parking lot, then energy can be fed from the PHEV to the grid. This can be done through the bi-directional dc-dc charger and the inverter as shown in Figure 2.5(e). Although attractive, this process can shorten the battery life. Thus it is not very common, unless the economic gain can be justified.

2.4 Optimal of Location of PV Based Charging Facility

Large-scale penetration of PHEVs can have a detrimental and destabilizing effect on the electric power grid [26]. With the variation in demand, the production of power can vary significantly. Since the initial deployment of PHEVs is assumed to be clustered to a particular neighborhood, many authors have focused their research on the study of distribution transformer impacts. Depending upon the time, place of vehicle charging, various charging methods and the charging power levels there could be several ramifications on the distribution network. The likelihood of observing local distribution infrastructure inadequencies significantly increases as higher voltages are used to reduce charging durations.

To facilitate the high penetration levels of PHEVs without adverse impact on the distribution equipment it is recommended to install PVCFs. Solar power is a reliable source for charging vehicles such as golf carts, scooters and utility vehicles at airports, educational institutions, workplaces etc. Many pilot projects are also underway to charge PHEVs from solar photovoltaic system. Co-benefits of large scale deployment of PHEVs and PV systems has been studied in. The study concludes that PV provides a potential source of midday generation capacity for PHEVs, while PHEVs provide a dispatchable load for low value or otherwise unusable PV generation during periods of low demand (particularly in the spring).

However, during the periods of high PV generation and low PHEV load conditions adverse situations would arise such as power flow inversion and voltage rise events. Since the distribution equipment are at an increasing risk of maloperation, this issue needs close attention with the increasing penetration of PVCFs. To address these issues optimal siting of PVCFs in a distribution network becomes very imperative. Several authors have proposed various methods for determining the optimal location of distributed generators in a distribution network. Optimization problems are defined based on driver behavior, distance traveled, battery capacities etc. [27] to decide the location of charging stations. In few cases National Household Travel Survey (NHTS) data is utilized to formulate a probabilistic model for locating (home, workplace or public charging) the place in real-time to charge PHEVs. Authors in [28] have proposed a 2 step methodology based on the active and reactive powers of PHEVs. The method is aimed at scheduling the location of PHEV charging such that the deviation in node voltages is minimized.

References [29] and [30] proposed a method to determine the PHEV charging load required for voltage regulation and compare the results for the different locations in the feeder. It can be inferred from the above review of literature that research communities are yet to come up with a robust solution for determining the optimal location of PVCFs in a distribution network.

This thesis proposes a new method for optimally siting PVCF with energy storage in a distribution network under stress due to heavy penetration of PHEVs. A PVCF is modeled with a novel ESS controller designed to intelligently keep the connected grid equipment within its operating limits. The controller algorithm uses past solar and EV load data as inputs to generate a reference for the power electronics interface, controlling power flow to/from all power sources and loads. By utilizing the developed model, the thesis evaluates the effect of integrating EVs on a power system and their impact on the voltage profile network due to heavy loading on previously loaded buses. It then works to offset the adverse effects on the distribution network with DG and energy storage. A multi-objective optimization problem is developed to obtain the optimal siting of charging stations, renewable energy sources (RES) and energy storage facilities. The optimization problem focuses on reducing power losses, improving voltage stability of the system and indirectly reducing the charging costs of EVs. The performance of the proposed heuristic method is demonstrated through a case study using an IEEE 30-bus microgrid.

Chapter 3 Modeling the Charging Facility

This chapter describes the detailed model of the PV based charging facility. The assumptions made, role of the battery controller and the battery control algorithm are presented. The proposed model is simulated using the SimPowerSystems toolbox of Matlab/Simulink and the results are presented.

3.1 Charging Facility Model

The charging facility is expressed as a power network of single-phase AC (200 V). Solar power with peak deliverable power roughly around mid-day is the on-site renewable energy DG. Incorporated with solar generation are the utility grid and several 150 V storage battery modules. The storage battery is controlled by the battery controller. It absorbs power from the PVs when generated PV power is surplus and supplies to the charging facility when generated PV power is insufficient to handle EV loads.

The proposed structure of the charging facility is shown in Figure 3.1. Power converter/inverter circuits are used to interface the all 3 power sources with the EV loads. The energy storage charge controller (possibly a DSP TMS320F28035) sits in the middle of the topology, determining the direction of power flow based on defined control algorithms. Siting the energy storage system and PV close to the charging loads provide better management and control of the integrated system and enable flexibility of operation in islanded and anti-islanded mode.

Developing the model for this thesis simulation required certain assumptions be made. These assumptions stated explicitly below such as size of charging facility, PV generation, and energy storage capacity could easily be modified and

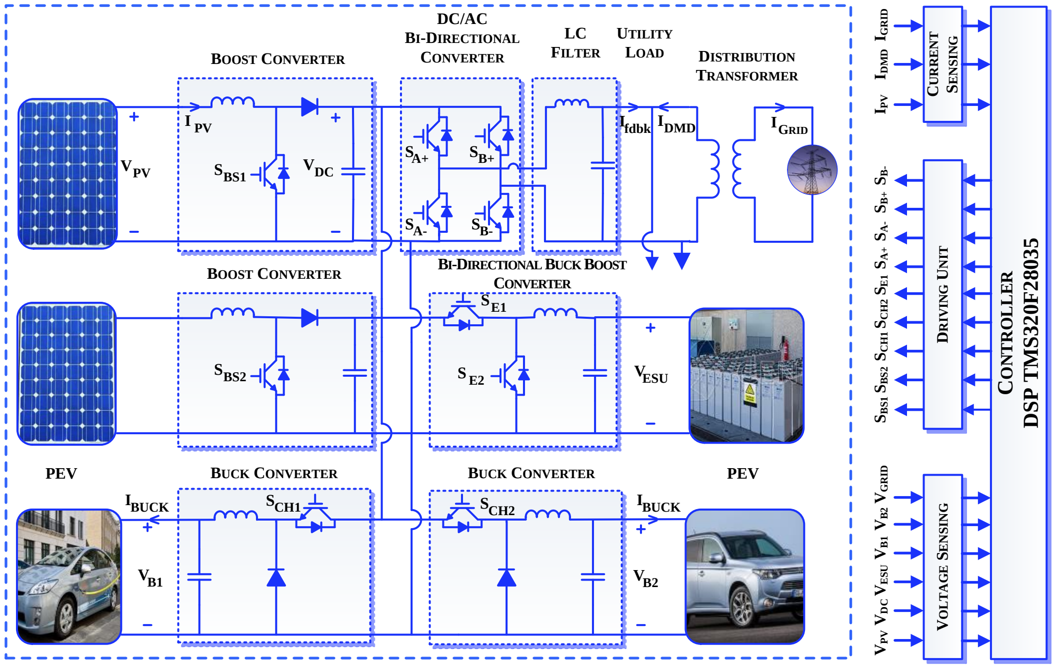

Figure 3.1: PHEV Charging Facility Model

scaled. Provided certain ratios specified below are kept within acceptable limits, the proposed solution is proven to yield consistent results.

Assumptions made for charging facility in the model:

1. Power requirements of charging facility at 100% capacity P_{load} = 1000 kW (A single Tesla supercharger for example can put out 120 kW depending on the EV battery SOC).

2. PV power generation available will supply an average of 30% of full load power during peak insolation; P_{pv}(at peak) = 300 kW.

3. From 20 h to 4 h, solar power generation is 0 W. It gets close to peak (300 kW) from 14 h to 15 h.

4. The energy storage system (ESS) consists of 20 giant modules of 10 kWh

each allowing total storage capacity $P_{battery}$ = 200 kW, 92% round-trip DC efficiency. Current rating: 5 A nominal, 8.5 A peak output.

5. The micro-grid is connected to the system power via a pole-mounted transformer. The pole-mounted transformer (primary 6.6 kV /secondary 240) changes the voltage from 6.6 kV to 240 V single-phase AC. The frequency of AC cycles is set to 60 Hz.

6. Solar power from PVs and the energy storage are DC power sources. In order to facilitate connection to the grid, power electronics are utilized to convert the DC power to single-phase AC. In the control strategy, the charging facility supplies most of the power from the PVs directly to the EVs. The balance of power required by the EV loads is then rationed between the energy storage and the grid depending on the algorithm objective function. The objective function of the energy storage controller works to minimize the adverse impact of EV charging on the connected grid.

The charging facility could be modeled to be as independent as possible but this would not be economical. Stochastic charging patterns and charging speed requirements of EV customers would require huge capital investment to implement. Also the excess power generated by the charging facility on slower days cause heavy penetration of power back to the grid, undermining the effort to relieve grid stress. The feasible solution remains a novel proportioning of grid power, solar energy, and energy storage covering the difference to ensure efficient power management of an entire system.

Table 3.1 shows an estimate of power charging requirements for an average PHEV. Depending on charging speed, power requirements per PHEV vary from 3.3 kW to 120 kW. Pricing and charge control strategies allow power to be deliv-

Table 3.1: Charging Requirements of an average 60 miles/charge PHEV

Charging time for 100 km of EV range	Power supply	Power	Voltage	Max. current
6-8 hours	Single phase	3.3 kW	230 V AC	16 A
3-4 hours	Single phase	7.4 kW	230 V AC	32 A
2-3 hours	Three phase	10 kW	400 V AC	16 A
1-2 hours	Three phase	22 kW	400 V AC	32 A
20-30 minutes	Three phase	43 kW	400 V AC	63 A
20-30 minutes	Direct current	50 kW	400-500 V DC	100-125 A
10 minutes	Direct current	120 kW	300-500 V DC	300-350 A

ered efficiently across all PHEV loads based on a defined set of parameters. This ensures the charging facility power requirements are kept within tolerable limits.

3.2 The Energy Storage System (ESS)

A wide range of technical solutions for ESS applications are described in [27]. Several studies on EV charging facilities have considered battery-based ESS technology [19-23]. This thesis ESS is modeled as a three-phase storage unit, with charge and discharge equations defined as

$$E(t + \Delta t) = E(t) - \Delta t \cdot \frac{P_d}{\eta_d} \text{ and} \tag{3.1}$$

$$E(t + \Delta t) = E(t) + \Delta t \cdot P_c \cdot \eta_c \ , \tag{3.2}$$

where P_d is the discharging power and P_c is the charging power of the ESS battery, respectively; $E(t)$ is the energy stored in the battery at time t ; Δt is the duration time of each interval. The two coefficients η_d and η_c are the discharging and charging efficiency, respectively. The operation of the battery system also takes into account power and energy constraints. The maximum power limits during charging/discharging can be described respectively by

$$0 \leq P_d(t) \leq P_d^{max} \text{ and} \tag{3.3}$$

$$0 \leq P_c(t) \leq P_c^{max} \ . \tag{3.4}$$

For simplicity, we will refer to P (in kW) to indicate the power flow in or out of the storage, including both phases of charging and discharging. The SOC limits of an ESS system can be described as:

$$SOC^{min} \leq SOC(t) \leq SOC^{max} \ , \tag{3.5}$$

where SOC^{min} and SOC^{max} are the minimum and maximum energy levels of the ESS, corresponding to the usable energy window (in kWh). The interval defined in Eqn. 3.5 is the usable energy window of the ESS battery. The energy limits of a battery is set by the application and battery technology used.

3.3 The ESS Controller

Integration of energy storage to the charging facility provides flexibility of power delivery with a potential to reduce grid stress. However, ESS control complicates management and control of system due to the large number variables under consideration. Two important aspects usually considered in designing energy management and control are generation-load power balance and state of charge (SOC) of the batteries. It is important to ensure charging facility load demands are met at all times especially during islanded. SOC is a measure of the short term capability of a battery or the amount of energy left compared to its energy on a full charge. In order to maintain battery health and lifetime, minimum and maximum SOC should be determined and considered for energy management and control design.

Quite a number of research work have been published related to energy management and control of microgrids with renewable energy and energy storage. In [30], the concept of using the energy storage system (ESS) within a public electric vehicle (EV) charging station for voltage regulation in a feeder was first highlighted. The ESS controller developed for this thesis utilizes a similar approach with an addition of time based predictive control into its objective function. By anticipating peak and off-peak periods for the solar energy resource and EV charging loads, the controller ensures the SOC of the ESS is at maximum just before peak EV charging begins. It also monitors the SOC relative to the current time and data (anticipated solar and EV charging loads) and uses its control algorithm to manage the ESS power charge/discharge rate to ensure enough power remains to serve through the entire period of peak EV charging and/low Solar insolation. The energy storage controller algorithm proposed here is developed and optimized to minimize power flow to and from the grid by controlling power delivery ratios within the intermittent PV, ESU and the charging station loads. The role of the battery controller can be summarized as follows:

1. The battery controller requires collected data of average Solar Insolation and EV charging station load patterns.

2. The battery controller ensures power demanded by the charging facility is delivered provided power demanded does not exceed its defined limit.

3. The battery controller dedicates 100% of power generated by the Solar Panel to the charging facility loads and balances the remainder between the ESS and the grid based on its internal algorithm .

4. The battery controller performs tracking of the current flow between the charging facility and the grid transformer. It attempts to minimize active power flowing to the charging facility from the grid during peak hours (cost of energy is highest) and maximize battery SOC through grid charging during off peak periods.

5. The controller absorbs surplus current from the PV when Solar generated is greater than load demanded by the charging facility.

6. The controller ensures the SOC of the battery is kept within its minimum and maximum limits.

7. The actual control is performed by a bidirectional dc-dc converter which takes its reference from the battery controller.

The bidirectional converter control is referenced to maintain dc link voltage at a specified value. The bidirectional converter has a buck-boost bidirectional topology and shown in Fig. 3.2. In the charging mode, the converter operates as a buck converter and controls the input voltage, which is the dc-link voltage. In the discharging mode, the converter operates as a boost converter and controls the output voltage, which is the dc link voltage. In both modes, the bidirectional converter control objective is to keep the dc link voltage at a specified voltage and also to regulate the charging/discharging current. The bidirectional converter control is implemented as a dual loop control with an external voltage control and internal current control. The control command to operate in charging or discharging mode comes from the energy management system (EMS).

The battery controller is implemented in Simulink/Matlab and results are shown over a 24 hour period. The written algorithm is readily adaptable on conversion for the DSP TMS320F2835 or other compatible DSP controller.

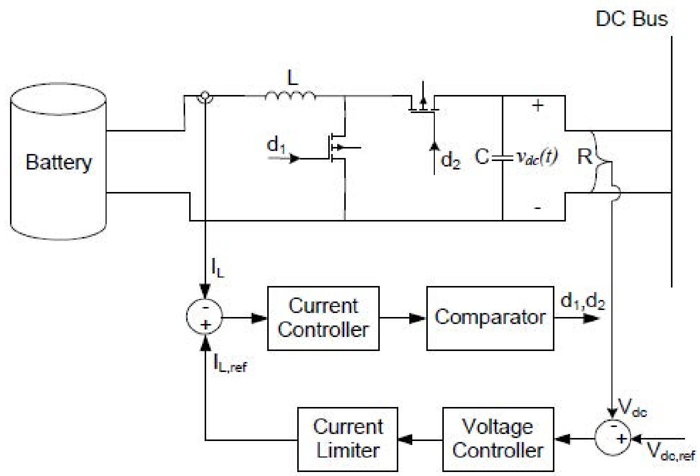

Figure 3.2: Bidirectional dc-dc converter topology and control

3.4 Battery Controller Algorithm

By directly controlling the charging and discharging of the storage unit through the power converters, the ESS controller defines power flow rates and directions between the main grid, solar energy resource and the charging facility. As defined in the controller role section, the ESS is forced to deliver full power to the charging facility load based on

$$P_{pv} + x \cdot P_{grid} + y \cdot P_{battery} = P_{load} \tag{3.6}$$

Since solar irradiation is practically non-existent at at night, P_{pv} is zero during this period and P_{load} must then be supplied from the grid and ESS. The values of x and y change in reaction to P_{pv}, load requirements, time and SOC of the ESS. Input and output parameters required by the ESS controller are defined below:

1. Controller input $\rightarrow$ Charging facility load pattern data, Solar Irradiation Data, Time, ESS SOC, P_{pv} and P_{load}.

2. Controller output $\rightarrow$ ESS charge or discharge toggle, ESS charge/discharge rate reference, charging facility islanded or anti-islanded mode.

0:00	*off peak*
1:00	*off peak*
2:00	*off peak*
3:00	*off peak*
4:00	*off peak*
5:00	*start peak*
6:00	*start peak*
7:00	*start peak*
8:00	*start peak*
9:00	*peak*
10:00	*peak*
11:00	*peak*
12:00	*peak*
13:00	*peak*
14:00	*peak*
15:00	*peak*
16:00	*peak*
17:00	*peak*
18:00	*end peak*
19:00	*end peak*
20:00	*end peak*
21:00	*end peak*
22:00	*end peak*
23:00	*end peak*

Figure 3.3: Hour Table for ESS Controller

Time incorporation to the thesis algorithm is a novel approach. The algorithm utilizes this parameter by placing time brackets into variable containers defined as *peak*, *off peak*, *start peak*, and *end peak*. As the clock progresses through each container, the algorithm calculates the time left for the current time to reach the next time period and adjusts the values of x and y to control charge/discharge rate.

Table 3.3 shows the time of day table used in this model. The *off peak* period (0 h to 4 h) marks a period of low costing grid power and little to no EV charging loads. The *start peak* period (5 h to 8 h) marks the start of both solar irradiation and EV charging according to input data provided. EV loads are mostly served on first come first serve basis with source power majorly from Solar and the main grid. During *peak* period (9 h to 17 h), EV loading is expected to rise to its highest point and drop steadily as seen by the EV charging station load curves. Maximum power from the PV panel is delivered to support these loads as the charging facility charges its connected EVs with its planned strategy. The ESS controller, calculating the time left till the *end peak* period rations its ESS left over energy by controlling power delivery rate from the ESS to the charging facility while forcing the grid to supply the remainder of required power. The ultimate goal of the ESS controller is to ensure the ESS contributes to a significant reduction in grid power contribution throughout the entire peak period. At *end peak*, the SOC of the ESS is expected to be at its all time low depending on EV loads. Left over loads are majorly charged from the grid with minor contribution from the ESS. The goal of the controller shifts again during *off peak*, controlling rate of charge from the grid to bring the battery SOC back to 0.95 just before the beginning of another *start peak*.

The controller starts this process by evaluating its input data. The referenced table also monitors the time of the day transition in the table, anticipating loads and power resources before its next time period. Figure 3.4 depicts the ESS control algorithm flowchart.

The cost of electricity in the controller algorithm is used to select the values of x and y which holds float values from 0 to 1.

The battery controller optimizes the power delivery rate from the ESU to maximize battery life while avoiding heavy loading on the connected grid.

3.5 Simulation and Results

The simulink model schematic is shown below in Figure 3.5. The battery controller algorithm is implemented in the battery control block which takes x and y values from its linked MATLAB optimization script. Simulation results are shown in Figure 3.6

Results demonstrate charging facility behavior over a 24 h period (0 to 82,800 seconds). Power delivered by the PV is obtained from existing solar insolation

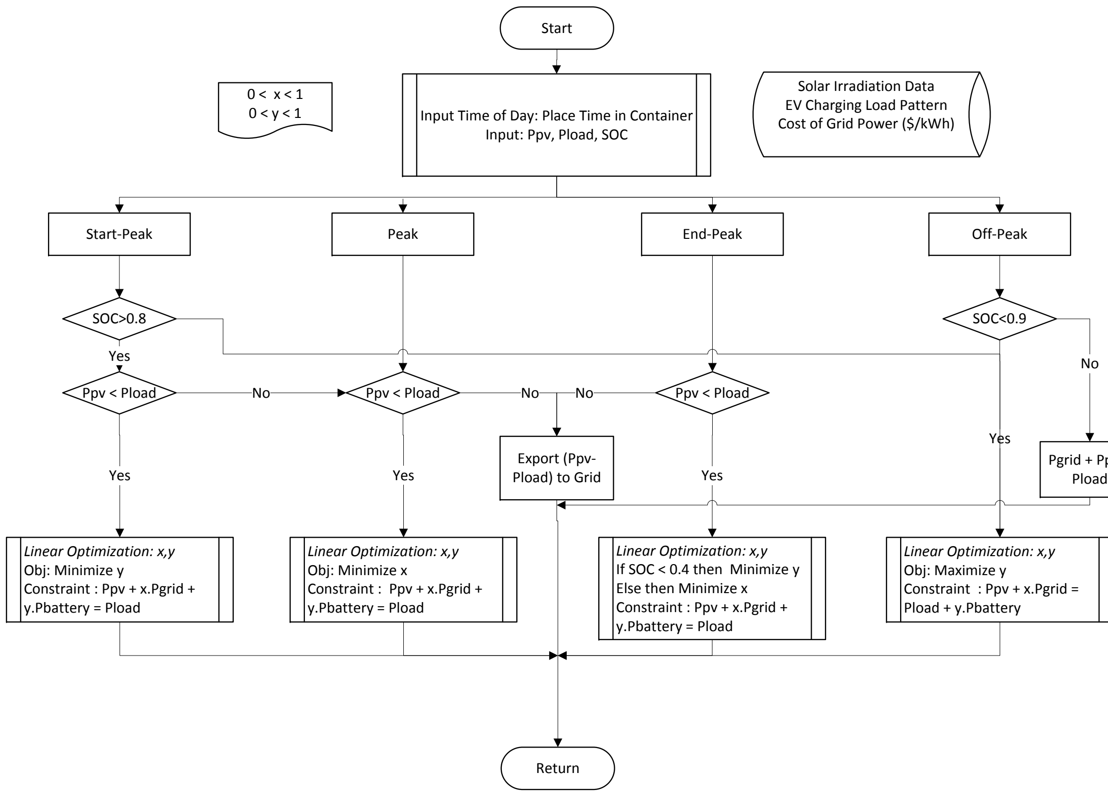

Figure 3.4: ESS Controller Algorithm Flowchart

data scaled to the thesis PV power assumptions defined earlier. As can be observed, PV power shown in the first subplot is maximum at 300 kW at mid-day around 15 h. Secondary power in the second subplot shows the power drawn from the grid to supplement the power delivered from the PV and ESS. The grid delivers enough power (shown as a negative quantity for power taken out of grid) to ensure EV load requirements are met. EV charging is assumed to follow a hypothesized trend for commercial EV charging stations, which peak at 9:30am (34200 seconds) as shown in the third subplot. The ESS shown in the fourth subplot attempts to provide power to the charging facility to meet charging loads during *startpeak* and *peak* periods. When power from the PV becomes greater

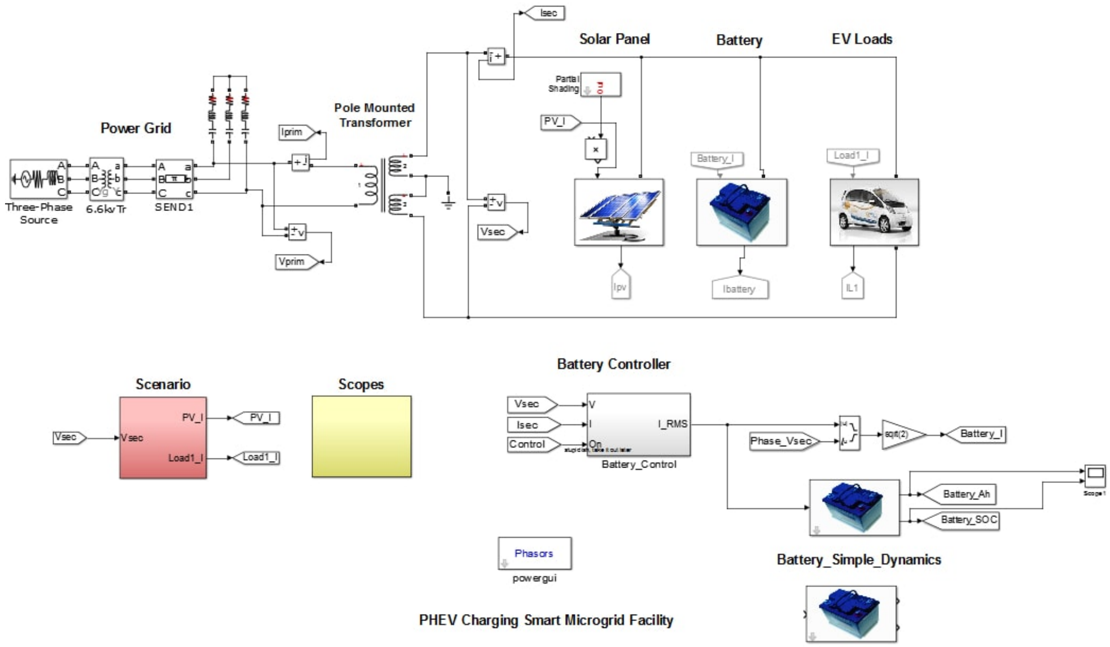

Figure 3.5: Implementation in Matlab/Simulink

than requirements from the charging facility, the ESS begins to draw power from the grid. The ESS controller caps power delivery limit for the ESS at 200 kW at all times to prevent damage to batteries. The battery SOC is shown to decrease when net power out of the ESS is positive(discharging) and vice-versa(charging). Finally, time of the day in seconds over a 24 h period is plotted as a reference for all above subplots.

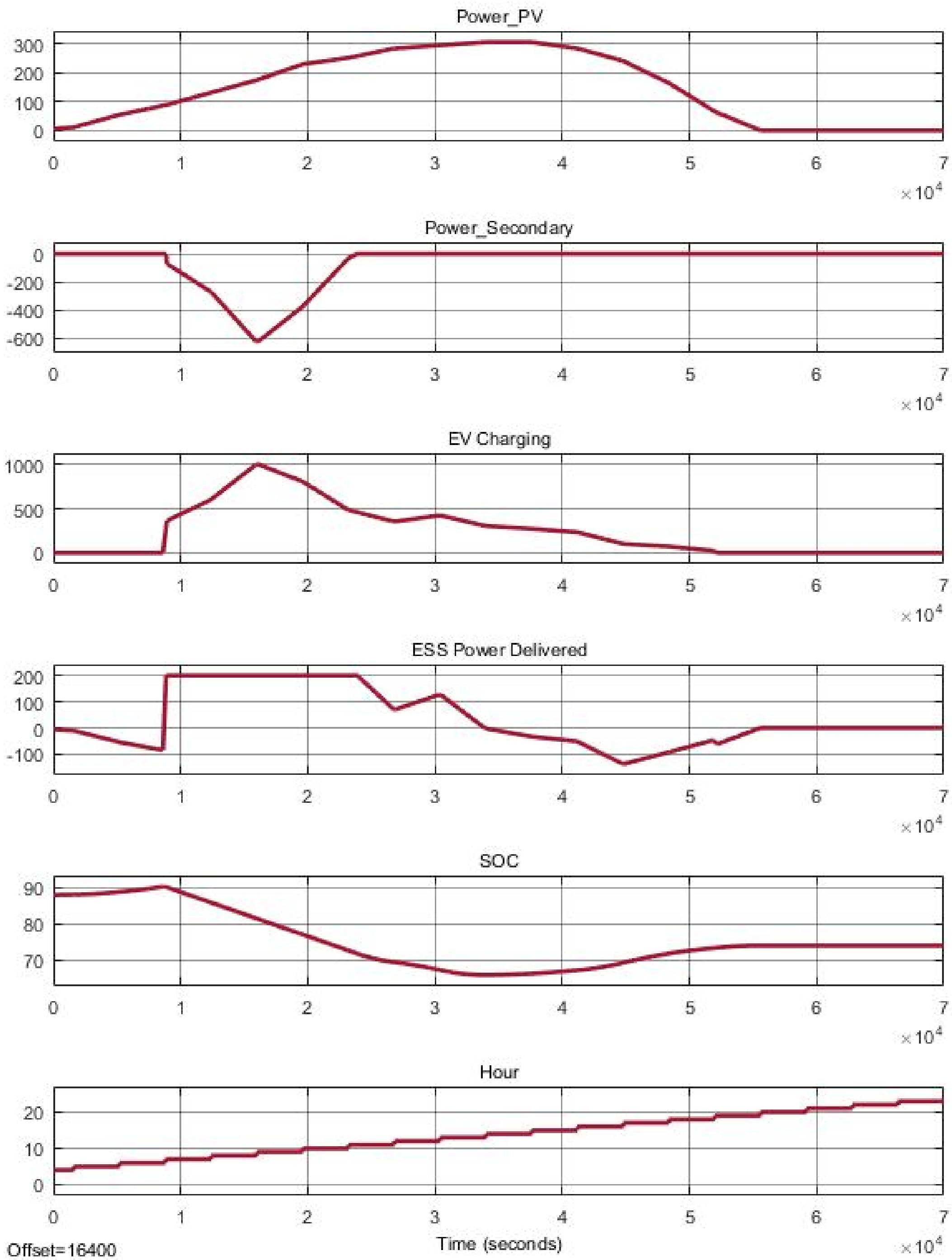

Figure 3.6: Simulation Results

Chapter 4 Proposed Method and Case Study

This chapter demonstrates the importance of optimally siting the charging facility load. An objective function with constraints is formulated for the Differential Evolution algorithm to find the optimal location of the charging facility. Finally, the proposed algorithm is tested on an IEEE 30 bus test case and results are presented.

4.1 IEEE 30 Bus Test Case

The IEEE 30 Bus Test Case used in this case study is obtained from a portion of the American Electric Power System in Midwestern US. A hard-copy data was provided by Iraj Dabbagchi of AEP and entered in IEEE Common Data Format by Rich Christie at the University of Washington in August 1993. This test case consists of 30 buses, five generators and three synchronous condensers. The model with buses at base 132kV and 32kV was modified to include transmission line limits which are utilized in this study.

A pictorial representation of the 30 bus case used to implement this study is shown in Figure 4.1. Fictional zones (displayed with colors) divide the bus system into six sections, each with capability of having its own charging facility. Zone selection for node placement were based on node proximity to neighboring nodes, and zone size criteria for a minimum of three nodes per zone. Table 4.1 shows the different bus parameters and results of a fast decoupled Newton Raphson power flow. Bus type 3, 2 and 0 represent slack, PV and PQ buses respectively.

Net power flow from the charging facility model in Chapter three used to simulate the charging station integration with the IEEE 30 bus system. To analyze

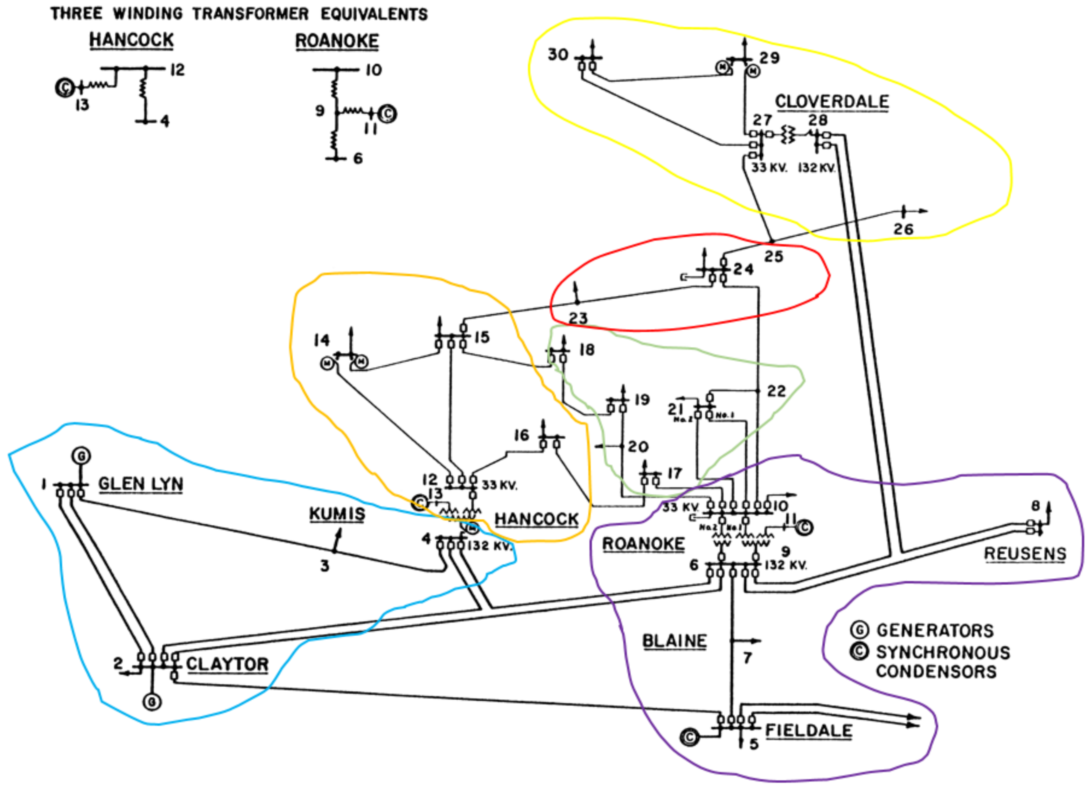

Figure 4.1: IEEE 30 Bus Test Case

the effects of the model integration over a 24 hour period, a healthy node is selected at random to place the facility. Figure 4.3 shows voltage magnitue plot as the charging facility draws power from the grid via a connection at node 17. The voltage magnitude at all 30 nodes are monitored from minimum to maximum loading over the 24 hour period with samples every four hours and the changes are plotted as faded lines. The lines grow from light to bold as EV penetration increases for easy visualization.

Fig. 4.3 to 4.5 show voltage drops across the grid due to increasing EV penetration. It is worthwhile to note the distinct reactions shown on each plot by the same load pattern. Fig. 4.5 shows significant voltage drop of about 0.08 pu at

Table 4.1: IEEE 30 Bus System Parameters

Bus Number	Bus kV	Bus Type	Bus Magnitude (PU)
1 Glen Lynn	132	3	1.06
2 Claytor	132	2	1.043
3 Kumis	132	0	1.021
4 Hancock	132	0	1.012
5 Fieldale	132	2	1.01
6 Roanoke	132	0	1.01
7 Blaine	132	0	1.002
8 Reusens	132	2	1.01
9 Roanoke	1	0	1.051
10 Roanoke	33	0	1.045
11 Roanoke	11	2	1.082
13 Hancock	1	0	1.071
16 Bus 16	33	0	1.045
19 Bus 19	33	0	1.026
20 Bus 20	33	0	1.03
21 Bus 21	33	0	1.033
22 Bus 22	33	0	1.033
23 Bus 23	33	0	1.027
25 Bus 25	33	0	1.017
26 Bus 26	33	0	1
27 Cloverdle	33	0	1.023
28 Cloverdle	32	0	1.007
29 Bus 29	33	0	1.003
30 Bus 30	33	0	0.992

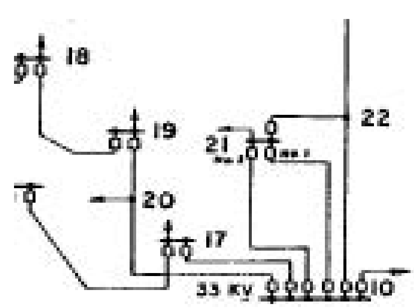

Figure 4.2: Zone 4 Pictorial Close-up View

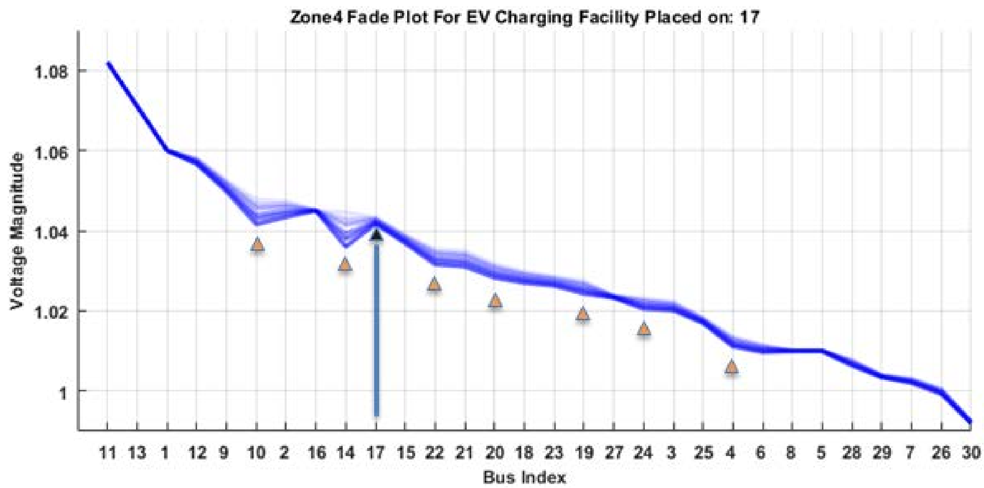

Figure 4.3: Effect of Increased EV Loading to Grid Voltage Profile: Node 17

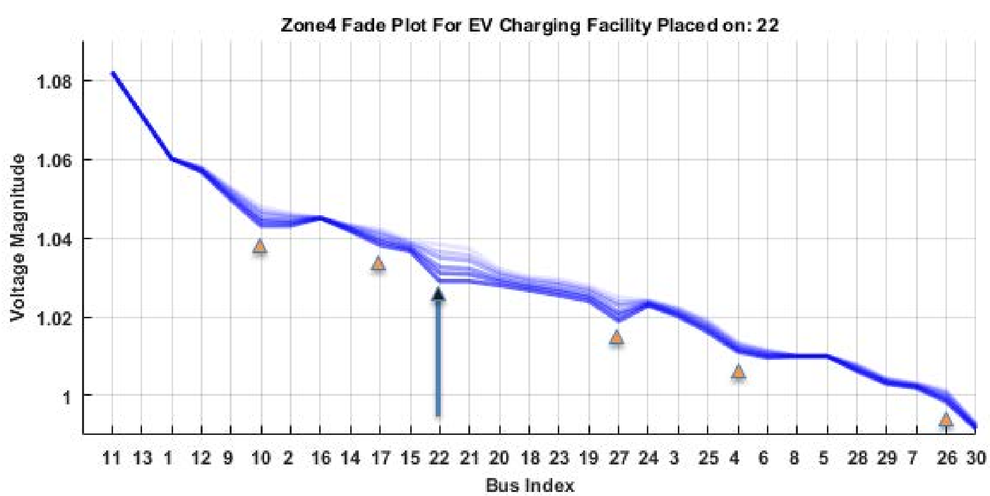

Figure 4.4: Effect of Increased EV Loading to Grid Voltage Profile: Node 22

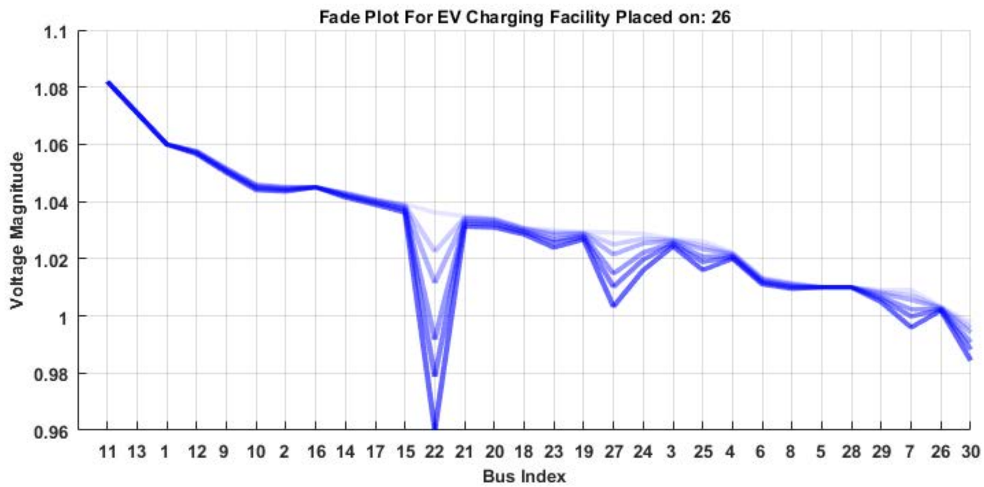

Figure 4.5: Effect of Increased EV Loading to Grid Voltage Profile: Node 26

node 22 for the EV loads connected at a separate bus (Node 26). Node 26 is shown to barely react to its directly connected load. A similar trend is also observed in Fig. 4.3 which shows Node 17 voltage stable at the expense of nodes 10 and 14 drop. These findings confirm that in a connected grid, neighboring nodes could be more affected by loading at a distant node than the node with direct connection to the load. Sometimes the directly loaded bus shows a voltage drop greater than its neighboring connected nodes as is the case in Fig. 4.4. This seemingly random phenomena is likely due to the nature of grid interconnectivity, transmission lines, and the interfacing power systems infrastructure which varies from system to system. Since every system is unique, selecting an optimal location that minimizes adverse effects while taking into consideration reasonable constraints becomes an issue requiring a robust solution. We solve this problem by creating an objective function encompassing our goal to minimize power losses. By utilizing non-resource intensive optimization techniques, we search the entire system space for an optimal location for the PVCF. To perform this study, we faced the challenge of collecting, processing and analyzing load flow data over a 24 hour time span. This challenge was resolved by sampling the data from the model every four hours. Data collected from samples show power ranging from maximum power drawn ($\approx$ 510 kW) to maximum power delivered to the grid ($\approx$ 50 kW) from/to the charging facility.

Multiple attempts have been made to find the optimal location of charging facilities on low voltage feeders. In [7] and [29] the authors attempt to find the optimal location of charging facilities but do not put into consideration the relative lack of flexibility in siting these facilities. Land constraints, easy accessibility among others are important factors that must be considered in an optimal siting problem. This thesis addresses the land constraint issue by implementing EV charging zones. The concept of zoning ensures the cost of charging facility placement in every major area covered by the system is properly evaluated. It also reduces the amount of work to be carried out every time a new charging facility is required to a different area in the same major grid. Although the system can be zoned to any requirement depending on the study, this thesis divided the system into six zones for the sake of simplicity. These zones are defined below

Charging Facility Zones and their respective nodes:

1. zone1= [1,2,3,4];
2. zone2= [5,6,7,8,9,10,11];
3. zone3= [12,13,14,15,16];
4. zone4= [17,18,19,20,21,22];
5. zone5= [23,24,25];
6. zone6= [26,27,28,29,30];

We show the effect of loading each zone with maximum drawn power from a PV powered charging facility without the ESS and with the ESS and its controller in 4.6. These results show the maximum loading effect a single charging facility

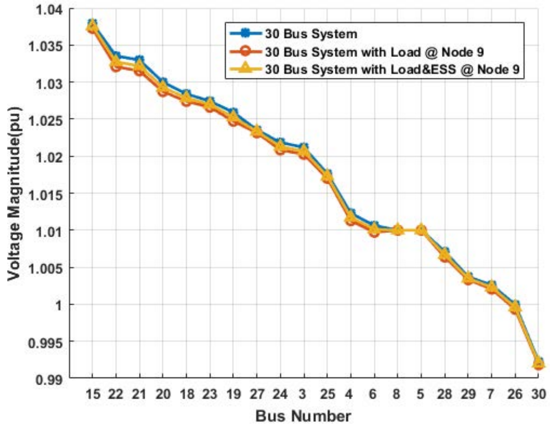

(a) System at Node 9

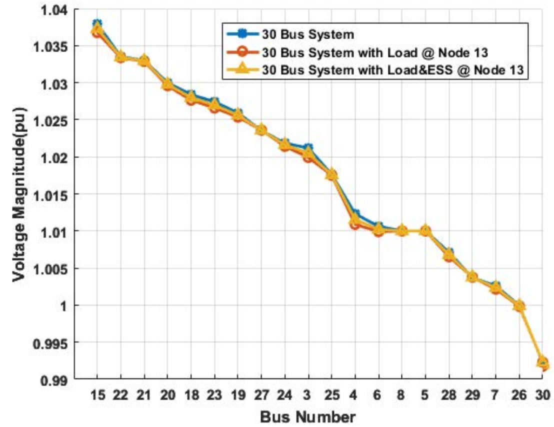

(b) System at Node 13

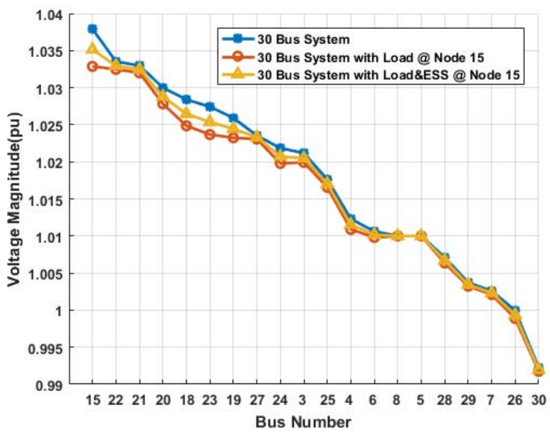

(c) System at Node 15

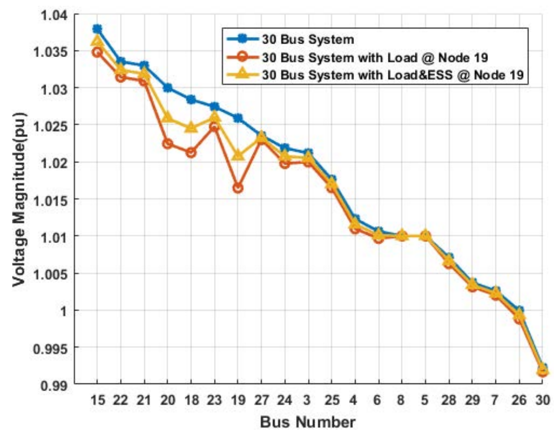

(d) System at Node 19

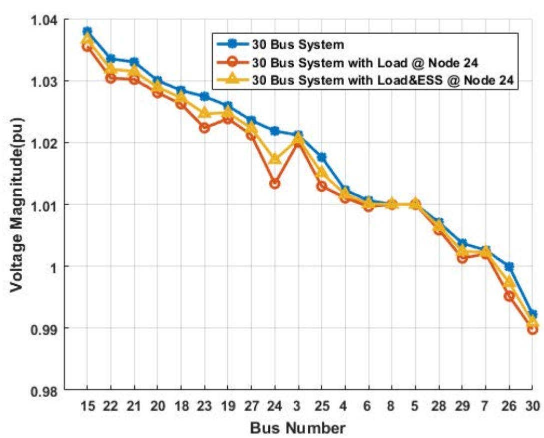

(e) System at Node 24

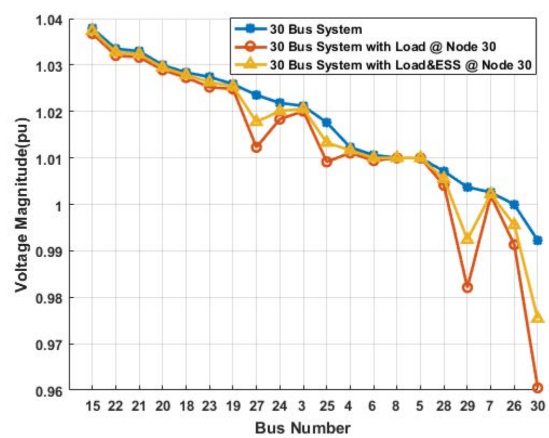

(f) System at Node 30

Figure 4.6: Effect of Max EV Loading Per Zone- With & Without ESS

placed at a random node could have on the power system. The significance of the plots is the proof that when sized correctly, the ESS and its controller were in 80% of the cases capable of keeping the grid node voltages from dropping below acceptable limits. In order to ensure all node voltages are kept within limits, additional steps must be taken to correctly site the PVCFs. Nodes not displayed were cut off from the figures due to a minuscule deviation from base case voltage.

4.2 Optimal Siting Problem

The aim of the proposed objective function is the reduction of power losses in the overall system through voltage stability improvement. Power loss improvements will indirectly result in a reduction of charging charging costs by reducing associated cost for unnecessary upgrades.

The objective function is formulated with the above goals as a weighted sum of three objectives

$$Min(F_T) = \tau f_1 + \beta f_2 + \zeta f_3 \, , \tag{4.1}$$

where τ, β and ζ are weighting coefficients adjusted according to the importance of each defined objective function. It was assumed from previous studies that $\tau = 0.5$; $\beta = 0.3$ and $\zeta = 0.2$. It is worth noting that each objective function in Eqn. 4.1 is normalized through a division by its base value calculated prior to the optimization process. This normalization makes the objective function dimensionless and it also prevents future scaling issues.

4.2.1 The Objective Functions

Power losses

The active power losses, f_1, of the network can be formulated as

$$f_1 = P_{loss} \ , \tag{4.2}$$

where P_{loss} can be calculated by

$$P_{loss} = \frac{1}{2} \sum_{t=1}^{24} \sum_{i=1}^{NB} \sum_{j=1}^{NB} G_{ij} [V_{i,t}^2 + V_{j,t}^2 - 2V_{i,t} V_{j,t} cos(\delta_{i,t} - \delta_{j,t}) \ . \tag{4.3}$$

These power losses can be decreased by effective management of the charging stations and proper control of the ESS.

Total voltage profile index

The total voltage profile index, f_2, of the network can be calculated by

$$f_2 = \sum_{t=1}^{24} \sum_{i=1}^{NB} |1 - V_{i,t}| \ . \tag{4.4}$$

Voltage at the load terminals can be kept within desired bounds by minimizing this index. Also, by introducing the solar powered DGs and EVs loads into the system, some portion of reactive and real power demanded by customers can be managed which in turn helps in decreasing system losses and improving the network voltage profile.

EVs charging and load supplying costs

This is the third objective function which can be calculated by

$$f_3 = \sum_{t=1}^{24} (P_{sub,t} * 1.2 * c_v) + f_{ch} - f_{dc} \ , \tag{4.5}$$

where

$$P_{sub,t} = \sum_{i=1}^{24} P_{d_{i,t}} + P_{loss,t} - \sum_{k=1}^{nPHEV} P_{dck,t}^{PHEV} + \sum_{k=1}^{nPHEV} P_{k,t}^{PHEV} - P_{pv,t} \ , \tag{4.6}$$

$$f_{ch} = \sum_{t=1}^{24} \sum_{m=1}^{Nst} P_{station,m,t} * c_p * T_{m,t} * (\frac{D_t}{D_{max}}) * (\frac{P_{M_{pv}}}{P_{pv,t}}) \ , \tag{4.7}$$

$$f_{dc} = \sum_{t=1}^{24} \sum_{m=1}^{Nst} P_{station,m,t} * 1.1 * c_v * t_{dispm,t} \ , \text{and} \tag{4.8}$$

$$P_{station} = P_{rate} * n_{PHEV} \ . \tag{4.9}$$

Eqn. 4.6 represents the amount of power which can be purchased from the substation. Eqn. 4.7 formulates the cost of EV charging in which the amount of charged power (on an hourly basis) is multiplied by the amount of tariff in order to improve charging profile. The tariff is multiplied by the amount of network demand and is divided by its maximum demand to improve the network load factor. In order to exploit the charging facility solar energy, the maximum power generated by the PVs is multiplied by the objective function and divided by the amount of hourly power. The goal is increasing the effectiveness of solar energy generated so that during a low demand period the power is stored in the ESS. Variable $T_{m,t}$ is the time it takes the m_{th} charging station to fully charge its connected EVs. The value of $T_{m,t}$ depends on the arriving EV's state of charge (SOC), the battery capacity of EVs and the power rate of each charging level [26]. Eqn. 4.8 gives revenue obtained by EV owners in a discharging period when the grid purchases the EV's energy at a price higher than normal tariff. This in turn aids in increasing the probability of selling EVs energy. Eqn. 4.9 formulates the amount of power consumed at the station to charge EVs.

4.2.2 Constraints

Demand supply balance

The active and reactive generated power should be equal to the demand and losses. This can mathematically be expressed as follows from [21]

$$P_{gi,t} = P_{di,t} + V_{i,t} \sum_{j=1}^{NB} V_{j,t} Y_{i,j} cos(\delta_{i,t} - \delta_{j,t} - \theta_{i,j}) \text{ and} \tag{4.10}$$

$$Q_{gi,t} = Q_{di,t} + V_{i,t} \sum_{j=1}^{NB} V_{j,t} Y_{i,j} sin(\delta_{i,t} - \delta_{j,t} - \theta_{i,j}) \ . \tag{4.11}$$

Voltage constraint

The phase angle and magnitude of bus voltages should be kept within allowable ranges

$$V_{min} \leq V_{i,t} \leq Vmax \text{ and} \tag{4.12}$$

$$\delta_{min} \leq \delta_{i,t} \leq \delta_{max} \ . \tag{4.13}$$

Generation constraint

The output power of the RES (PV) in a period t should be kept within its minimum and maximum power limits

$$P_{min}^{RES} \leq P_{i,t}^{RES} \leq P_{max}^{RES} \ . \tag{4.14}$$

Zoning constraints

Selection of a connection node for the EV charging facility to satisfy above constraints must be confined to certain defined physical boundaries called zones.

4.3 Differential Evolution Algorithm

The single-objective evolutionary algorithm proposed by Price and Storn in 1995 draws upon ideas from several genetic algorithms and evolutionary methods. One of them is a relatively new element to the general class of evolutionary methods called differential evolution. As other evolutionary methods, DE is a population based technique for finding global optima. The three main operators of DE are mutation, crossover and selection. Much of the power of this method is resulted from a very useful mutation operator that is simple and effective. Mutations are obtained by computing the difference between two randomly chosen solution vectors in the population and adding a portion of this difference to a third randomly chosen solution vector to obtain a candidate vector. The resulting magnitude of the mutation in each of the variables is different and close to optimal. . If there is no mutation, offspring is taken after crossover (or copy) without any change. If mutation is performed, part of chromosome is changed. If mutation probability is 100%, whole chromosome is changed, if it is 0%, nothing is changed. An additional two parameters adopted in DE are crossover CR and mutation F. CR controls the influence of the parent in the generation of the offspring. Higher values mean less influence of the parent in the features of its offspring. If there is a crossover, offspring is made from parts of parents' chromosome. If crossover probability is 100%, then all offspring is made by crossover. If it is 0%, a whole new generation is made from exact copies of chromosomes from old population. F scales the influence of the set of pairs of solutions selected to calculate the mutation value. This method has been known as one of the most powerful evolutionary algorithms for real number function optimization problems.

The use of Differential evolution techniques in power systems has mainly been to solve an optimal power flow (OPF) problem. An important interest of many utilities, the approach employs the algorithm for an optimal setting of OPF control variables. Because the OPF problem is a highly non-linear and multi-modal optimization problem, local optimization techniques are not suitable for such problem. Moreover, there is no criterion to decide whether a local solution is also the global solution causing techniques such as the DE to gain popularity for use in OPF problems.

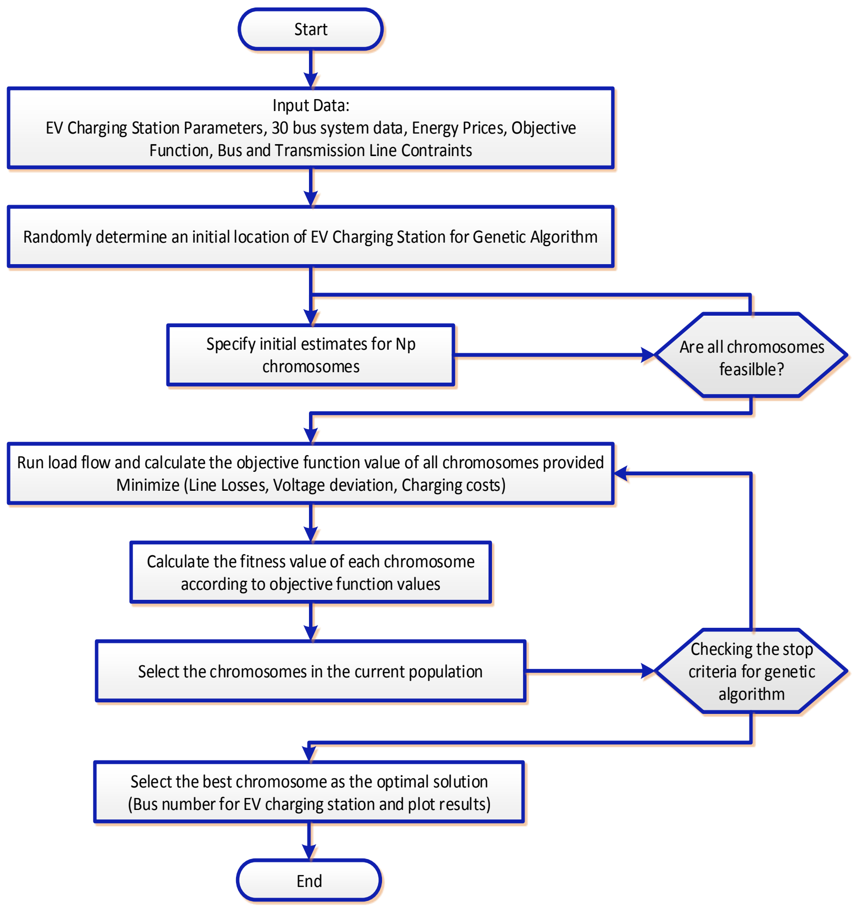

Figure 4.7: DE Algorithm Flowchart for Optimal Location Search

The flowchart utilized for finding a global optima for the charging facility is shown in Fig. 4.7. Table 4.2 shows the parameters utilized for the DE optimization. These parameters were obtained from previous literature and trial methods. Results of simulations showing optimal nodes for both maximum loading and excess PV injection from the model are shown in Tables 4.3 and 4.4. It is worth-

Table 4.2: DE Optimization Parameters

NP	CR	F	No. of Iterations	D
30	0.7	0.5	35	Node count per Zone

Table 4.3: Results from DE Simulations Case: Max Power

Zone	Optimal Node	VMag(pu)@ Optimal Node	Net Power Loss(MVA)
1	2	1.0175	13.8836
2	6	0.9980	15.8909
3	13	1.0270	16.2983
4	22	1.0070	16.6927
5	24	1.0220	16.8455
6	28	1.0000	15.7701

Table 4.4: Results from DE Simulations Case: Min Power

Zone	Optimal Node	VMag(pu)@ Optimal Node	Net Power Loss(MVA)
1	3	1.0141	14.0379
2	8	1.0100	14.1094
3	13	1.0450	13.8554
4	17	1.0403	13.7451
5	24	1.0350	13.7282
6	28	1.0020	13.7195

while noting that the optimization selected different optimal nodes for injection and loading cases (Zones 2 and 4). Results suggest that the grid reacts differently to injection vs loading by the PVCF model.

Fig. 4.9 and 4.10 show total power lost in the transmission lines for both the maximum loading and injection cases. We plot the power loss in transmission lines for all possible locations (bus 2 to 30)of our single charging facility. A direct comparison between Nodes 28 and 30 (Zone 6) show show optimal placement having a potential to reduce line losses by 0.25 MW + 0.9805 MVA.

Finally net real and reactive power generated by the case system to meet the charging facility needs and service the resulting increase in transmission line

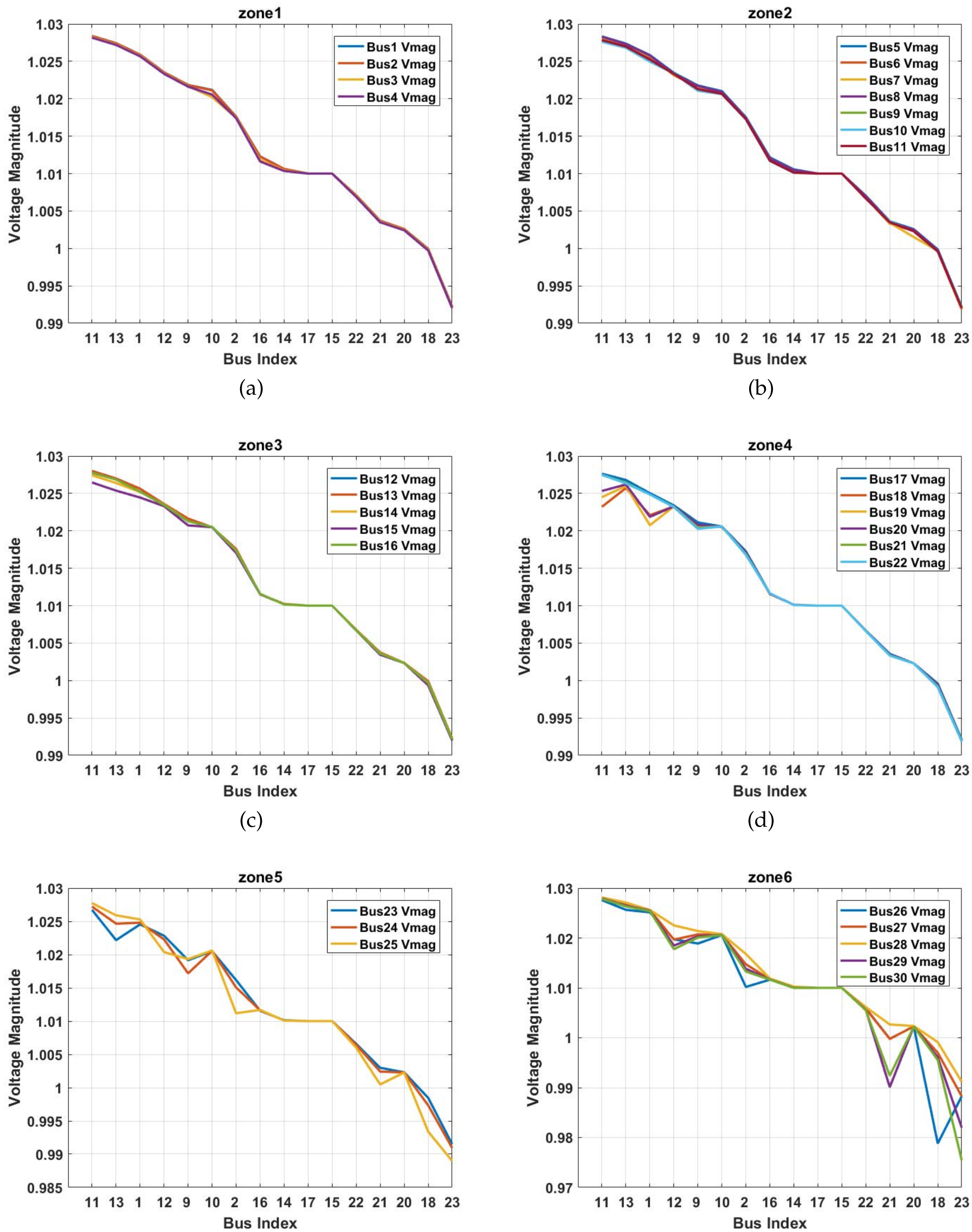

(a) (b)

(c) (d)

(e) (f) 30

Figure 4.8: Voltage Magnitude Plots with EV charging confined to each of the 6 Zones

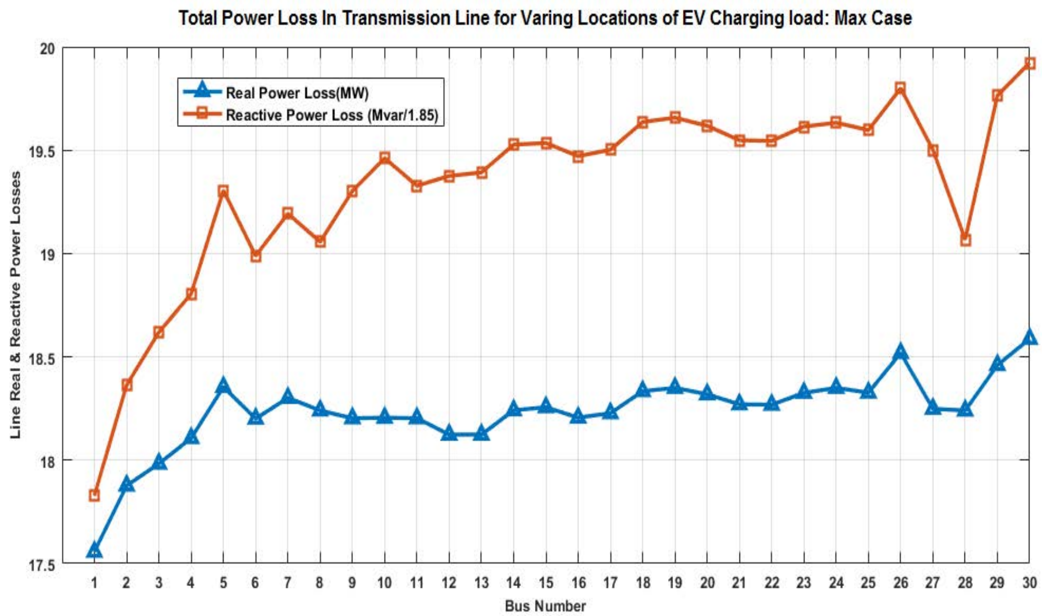

Figure 4.9: Total Power Lost in Transmission lines for Various Charging Station Locations: EV Loading

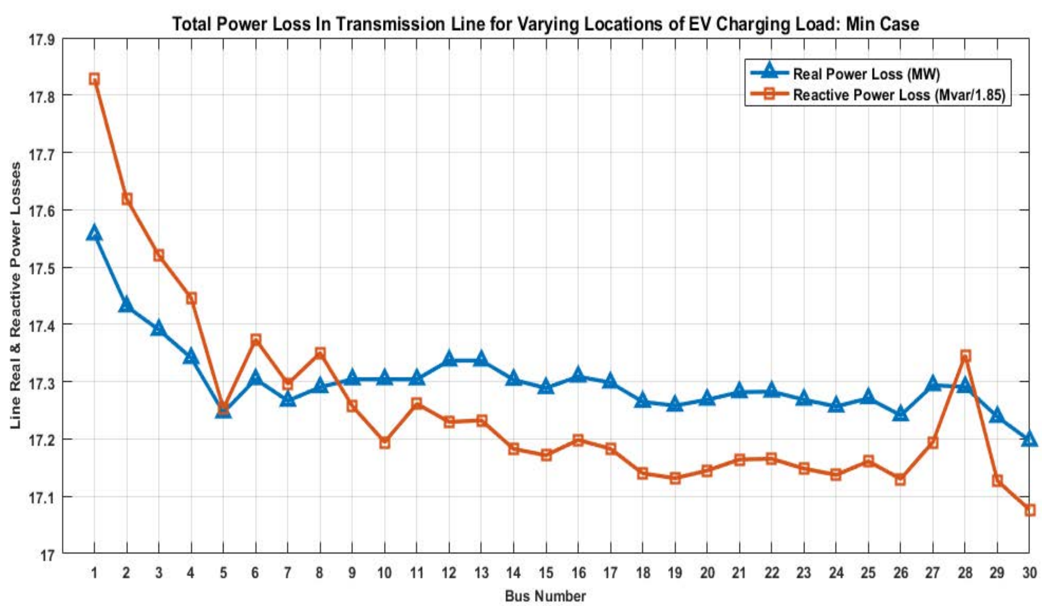

Figure 4.10: Total Power Lost in Transmission lines for Various Charging Station Locations: PV Injection

power loss is shown. It is worth noting the significant effect EV penetration and node selection has on reactive power loss in comparison to real power losses. This finding prompts an investigation into the use of reactive power compensation at selected nodes to as a method of further reducing the effects of EV penetration from DC fast charging.

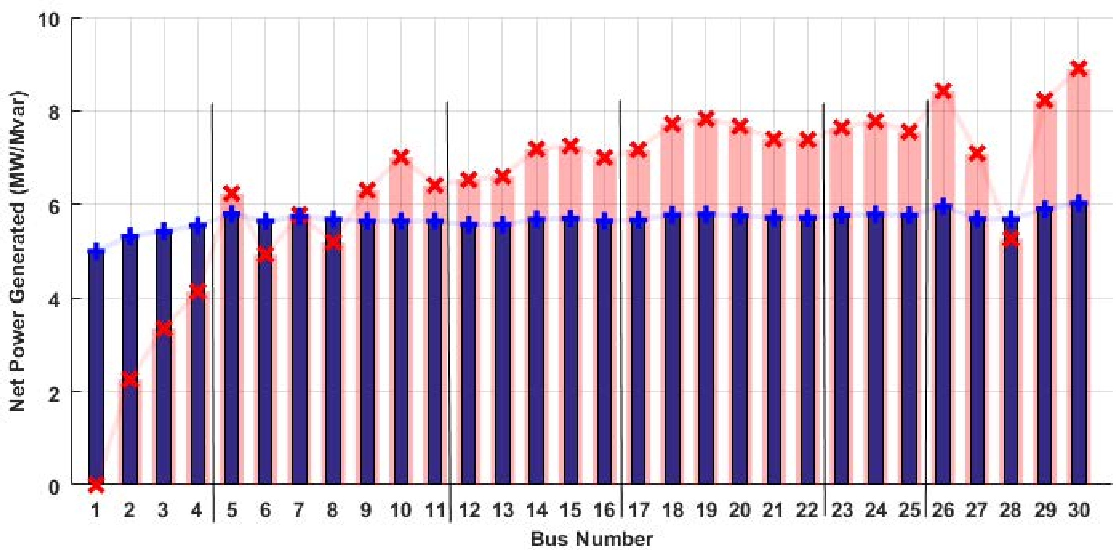

Figure 4.11: Total Power Consumption of the System for various locations of the EV Charging Facility

Chapter 5 Conclusions and Future Work

5.1 Conclusion

This thesis proposed a new method for optimally siting PVCFs with energy storage in a distribution network under stress due to heavy penetration of PHEVs. The development of an efficient ESS controller algorithm contributes to the recent popular use of energy storage to smooth the impact of the PV and the large EV loads on the power grid. It introduced the looming constraint of a relative lack of flexibility in siting the charging facilities which must be easily accessible to the EV drivers by zoning the case study system. The objective function was confined to each zone and the DE optimization algorithm was modified to run simultaneously across 6 zones, each zone simulated as a separate entity.

Results presented from simulations show an average of 2 MVA reduction in total power lost in transmission lines as a direct result of selective placement of the charging facilities. More importantly, optimally siting the charging facility ensured power loading on the case study transmission line were kept below their defined limits which was not the case with random siting. It was found that with EV stations at multiple locations, the cumulative power level for voltage support from the grid was always higher than the optimal charging load obtained with an EV station at a single location. To solve this problem, DG's must be optimally placed relative to the charging facilities and a more complex multi-objective optimization problem must be solved.

5.1.1 Future Work

Investigations into simultaneous installations of one or more charging facility per zone is inevitable considering current refueled interest in EV's and the resulting increase in charging station networks to service them. This thesis acknowledges that one or two superchargers with or without PV's or other form of DG will be placed at serviceable locations where convenience is top priority. Future studies must access the impact these superchargers capable of drawing up to 120 kW (in under an hour) have on the grid and develop new algorithms to optimally place multi-level charging stations relative to these superchargers.

References

[1] R. C. G. II, L. Wang, and M. Alam, “The impact of plug-in hybrid electric vehicles on distribution networks: A review and outlook,” *Renewable and Sustainable Energy Reviews*, vol. 15, no. 1, pp. 544 – 553, 2011.

[2] S. Shao, M. Pipattanasomporn, and S. Rahman, “Challenges of PHEV penetration to the residential distribution network,” in *Power Energy Society General Meeting, 2009. PES ’09. IEEE*, July 2009, pp. 1–8.

[3] G. Carli and S. Williamson, “Technical considerations on power conversion for electric and plug-in hybrid electric vehicle battery charging in photovoltaic installations,” *Power Electronics, IEEE Transactions on*, vol. 28, no. 12, pp. 5784–5792, Dec 2013.

[4] X. Li, L. A. C. Lopes, and S. Williamson, “On the suitability of plug-in hybrid electric vehicle (PHEV) charging infrastructures based on wind and solar energy,” in *Power Energy Society General Meeting, 2009. PES ’09. IEEE*, July 2009, pp. 1–8.

[5] P. Goli and W. Shireen, “Pv integrated smart charging of PHEVs based on DC link voltage sensing,” *Smart Grid, IEEE Transactions on*, vol. 5, no. 3, pp. 1421–1428, 2014.

[6] Z. Liu, F. Wen, and G. Ledwich, “Optimal siting and sizing of distributed generators in distribution systems considering uncertainties,” *IEEE Transactions on Power Delivery*, vol. 26, no. 4, pp. 2541–2551, Oct 2011.

[7] M. H. Moradi, M. Abedini, S. R. Tousi, and S. M. Hosseinian, “Optimal siting and sizing of renewable energy sources and charging stations simultaneously

based on differential evolution algorithm," *International Journal of Electrical Power & Energy Systems*, vol. 73, pp. 1015 – 1024, 2015.

[8] K. Liu and J. Makaran, "Design of a solar powered battery charger," in *Electrical Power Energy Conference (EPEC), 2009 IEEE*, Oct 2009, pp. 1–5.

[9] "The potential of photovoltaic carports to cover the energy demand of road passenger transport," *Progress in Photovoltaic: Research and Applications*, vol. 20, no. 0, pp. 639 – 649, 2011.

[10] J. Ingersoll and C. Perkins, "The 2.1 kW photovoltaic electric vehicle charging station in the city of santa monica, california," in *Photovoltaic Specialists Conference, 1996., Conference Record of the Twenty Fifth IEEE*, May 1996, pp. 1509–1512.

[11] F. Locment, M. Sechilariu, and C. Forgez, "Electric vehicle charging system with PV grid-connected configuration," in *Vehicle Power and Propulsion Conference (VPPC), 2010 IEEE*, Sept 2010, pp. 1–6.

[12] L. S, "Solar electricity as a fuel for light vehicles," in *In: Proceedings of the 2009 American solar energy society annual conference, Boulder, CO*, 2009.

[13] P. J. Tulpule, V. Marano, S. Yurkovich, and G. Rizzoni, "Economic and environmental impacts of a PV powered workplace parking garage charging station," *Applied Energy*, vol. 108, no. 0, pp. 323 – 332, 2013.

[14] D. P. B. III, "Solar-to-vehicle (S2V) systems for powering commuters of the future," *Journal of Power Sources*, vol. 186, no. 2, pp. 539 – 542, 2009.

[15] Q. Zhang, T. Tezuka, K. N. Ishihara, and B. C. Mclellan, "Integration of PV power into future low-carbon smart electricity systems with EV and HP in kansai area, japan," *Renewable Energy*, vol. 44, no. 0, pp. 99 – 108, 2012.

[16] P. Denholm, M. Kuss, and R. M. Margolis, “Co-benefits of large scale plug-in hybrid electric vehicle and solar PV deployment,” *Journal of Power Sources*, vol. 236, no. 0, pp. 350 – 356, 2013.

[17] U. D. of Transportation, “Summary of travel trends : 2009 household travel survey.” [Online]. Available: http://nhts.ornl.gov/2009/pub/stt.pdf

[18] M. Rutherford and V. Yousefzadeh, “The impact of electric vehicle battery charging on distribution transformers,” in *Applied Power Electronics Conference and Exposition (APEC), 2011 Twenty-Sixth Annual IEEE*, March 2011, pp. 396–400.

[19] R. C. G. II, L. Wang, and M. Alam, “The impact of plug-in hybrid electric vehicles on distribution networks: A review and outlook,” *Renewable and Sustainable Energy Reviews*, vol. 15, no. 1, pp. 544 – 553, 2011.

[20] S. Shao, M. Pipattanasomporn, and S. Rahman, “Challenges of PHEV penetration to the residential distribution network,” in *Power Energy Society General Meeting, 2009. PES ’09. IEEE*, July 2009, pp. 1–8.

[21] J. Zhao, S. Kucuksari, E. Mazhari, and Y.-J. Son, “Integrated analysis of high-penetration PV and PHEV with energy storage and demand response,” *Applied Energy*, vol. 112, no. 0, pp. 35 – 51, 2013.

[22] M. Erol-Kantarci and H. Mouftah, “Management of PHEV batteries in the smart grid: Towards a cyber-physical power infrastructure,” in *Wireless Communications and Mobile Computing Conference (IWCMC), 2011 7th International*, July 2011, pp. 795–800.

[23] G. Carli and S. Williamson, “Technical considerations on power conversion for electric and plug-in hybrid electric vehicle battery charging in photo-

voltaic installations," *Power Electronics, IEEE Transactions on*, vol. 28, no. 12, pp. 5784–5792, Dec 2013.

[24] M. Giannouli and P. Yianoulis, "Study on the incorporation of photovoltaic systems as an auxiliary power source for hybrid and electric vehicles," *Solar Energy*, vol. 86, no. 1, pp. 441 – 451, 2012.

[25] X. Li, L. A. C. Lopes, and S. Williamson, "On the suitability of plug-in hybrid electric vehicle (PHEV) charging infrastructures based on wind and solar energy," in *Power Energy Society General Meeting, 2009. PES '09. IEEE*, July 2009, pp. 1–8.

[26] S. W. Hadley, "Evaluating the impact of plug-in hybrid electric vehicles on regional electricity supplies," in *Bulk Power System Dynamics and Control - VII. Revitalizing Operational Reliability, 2007 iREP Symposium*, Aug 2007, pp. 1–12.

[27] G. Wang, Z. Xu, F. Wen, and K. P. Wong, "Traffic-constrained multiobjective planning of electric-vehicle charging stations," *IEEE Transactions on Power Delivery*, vol. 28, no. 4, pp. 2363–2372, Oct 2013.

[28] X. Lu, N. Liu, Q. Chen, and J. Zhang, "Multi-objective optimal scheduling of a DC micro-grid consisted of PV system and EV charging station," in *2014 IEEE Innovative Smart Grid Technologies - Asia (ISGT ASIA)*, May 2014, pp. 487–491.

[29] D. Meyer, J. Choi, and J. Wang, "Increasing EV public charging with distributed generation in the electric grid," in *Transportation Electrification Conference and Expo (ITEC), 2015 IEEE*, June 2015, pp. 1–6.

[30] F. Marra, G. Y. Yang, C. Traeholt, E. Larsen, J. Ostergaard, B. Blazic, and W. Deprez, "EV charging facilities and their application in LV feeders with

photovoltaics," *IEEE Transactions on Smart Grid*, vol. 4, no. 3, pp. 1533–1540, Sept 2013.